

Copyright
by
Jared Allison
2017

The Thesis committee for Jared Allison
Certifies that this is the approved version of the following thesis:

**Powder Bed Fusion Metrology for Additive
Manufacturing Design Guidance**

**APPROVED BY
SUPERVISING COMMITTEE:**

Carolyn Seepersad, Supervisor

Richard Crawford

**Powder Bed Fusion Metrology for Additive
Manufacturing Design Guidance**

by

Jared Allison

Thesis

Presented to the Faculty of the Graduate School of

The University of Texas at Austin

In Partial Fulfillment

of the Requirements

For the Degree of

Master of Science in Engineering

The University of Texas at Austin

August 2017

Powder Bed Fusion Metrology for Additive

Manufacturing Design Guidance

by

Jared Allison, MSE

The University of Texas at Austin, 2017

SUPERVISOR: Carolyn Seepersad

The benefits afforded by the use of additive manufacturing (AM) are diminished due to limited understanding of the various AM processes. Design for additive manufacturing (DFAM) guidelines can be generated through metrology studies using test parts to characterize specific processes and inform designers. Polymer selective laser sintering (SLS) is an AM process that can be used to create geometrically complex, end-use parts. However, no DFAM guidelines exist for polymer SLS that are both comprehensive and statistically robust.

A test part is designed for polymer selective laser sintering (SLS) that incorporates an array of geometric features. The part is comprehensive, including a variety of different features of interest to a designer. Many copies of the test part are built in a factorial-style metrology study, while varying different input parameters. The part is built in multiple materials, build orientations, locations within the build chamber, and on different machines to assess the variation attributed to each processing parameter. Multiple replicates are created at each point in the experimental design to add statistical robustness to the results.

Both resolution and accuracy are investigated based on the features of the test part. Upon measurement of the test parts, tolerances and design allowables could be established and compiled into a set of design guidelines for SLS. The design guidelines are structured to include varying levels of detail depending on the intent of the designer implementing them. Lastly, the guidelines are assembled into an online web-based tool that allows them to be accessed freely. Using the web tool, designers can realize parts with fewer mistakes and iterations in the design process.

Table of Contents

CHAPTER 1 INTRODUCTION.....	1
1.1 MOTIVATION.....	1
1.2 SLS PROCESS OVERVIEW	2
1.3 REQUIREMENTS FOR METROLOGY TEST PART.....	3
1.4 PREVIOUS WORK	4
1.5 RESEARCH GOALS	6
CHAPTER 2 DESIGN OF A TEST PART	8
2.1 INTRODUCTION	8
2.2 SLS TEST PART DESIGN	8
2.3 FEATURES CONSIDERED.....	10
CHAPTER 3 OVERVIEW OF METROLOGY STUDY	15
3.1 INTRODUCTION	15
3.2 MATERIAL	17
3.3 ORIENTATION WITHIN BUILD CHAMBER	18
3.4 LOCATION WITHIN BUILD CHAMBER	19
3.5 MACHINE VARIABILITY	21
CHAPTER 4 MEASUREMENT PROCEDURE.....	23
4.1 INTRODUCTION	23
4.2 MEASUREMENT TECHNIQUES	23

4.2.1	Surface Roughness.....	23
4.2.2	Linear Accuracy.....	24
4.2.3	Gap Accuracy as a Function of Wall Thickness.....	25
4.2.4	Hole Diameter as a Function of Wall Thickness	26
4.2.5	Thin Walls.....	26
4.2.6	Thin Rods.....	27
4.2.7	Hinges	28
4.2.8	Lettering.....	28
4.2.9	Snap Fits.....	29
4.3	GAGE REPEATABILITY AND REPRODUCIBILITY (GAGE R&R).....	29
CHAPTER 5 DESIGN GUIDELINES.....		31
5.1	INTERPRETATION OF RESULTS	31
5.1.1	Resolution	31
5.1.2	Accuracy	32
5.1.3	Significant Effects.....	32
5.1.4	Mean Differences.....	33
5.2	DESIGN GUIDELINES BY FEATURE TYPE	34
5.2.1	Surface Roughness.....	34
5.2.2	Linear Accuracy.....	36
5.2.3	Gap Accuracy as a Function of Wall Thickness.....	39
5.2.4	Hole Diameter as a Function of Wall Thickness	42
5.2.5	Thin Walls.....	45

5.2.6 Thin Rods.....	50
5.2.7 Hinges	53
5.2.8 Lettering.....	54
5.2.9 Snap Fits.....	57
5.3 MACHINE VARIABILITY	58
CHAPTER 6 PUBLIC ACCESSIBILITY OF DESIGN GUIDELINES	62
6.1 INTRODUCTION	62
6.2 WEB TOOL.....	62
6.3 INTERACTIVE CAPABILITY	64
CHAPTER 7 CLOSURE.....	67
7.1 SUMMARY	67
7.2 IMPLICATIONS	69
7.3 FUTURE WORK	71
APPENDIX A	73
REFERENCES.....	75

List of Tables

Table 1:	Polymer test cube feature ranges [10].....	11
Table 2:	Comparison of different test parts, including dimensions and feature density [10].....	14
Table 3:	Metrology study experiment design.....	16
Table 4:	Convention used for describing orientation of test cubes within the build chamber.....	19
Table 5:	Experiment design including machine variability	22
Table 6:	Convention used to determine resolution of lettering features	28
Table 7:	Gage R&R results for linear accuracy	30
Table 8:	Interpretation of significant effects tables.....	33
Table 9:	Significant effects visualization example	33
Table 10:	Significant effects for linear accuracy.	38
Table 11:	Significant effects for gap accuracy.....	41
Table 12:	Hole diameter resolution as a function of wall thickness for all test cubes	44
Table 13:	Significant effects for hole accuracy.....	44
Table 14:	Thin wall resolution for all test cubes.....	47
Table 15:	Significant effects for thin wall accuracy	48
Table 16:	Resolution of thin walls built in the XY orientation.....	49
Table 17:	Resolution of thin walls built in the XZ orientation	50
Table 18:	Resolution of thin walls built in the YZ orientation	50
Table 19:	Resolution of supported rods for all test cubes.....	51

Table 20: Resolution of unsupported rods with an aspect ratio of 10 for all test cubes .	52
Table 21: Resolution of unsupported rods with an aspect ratio of 5 for all test cubes ...	52
Table 22: Hinge resolution at shaft clearances of 0.6 and 1.0mm for all test cubes.....	53
Table 23: Resolution of embossed lettering for all test cubes	56
Table 24: Resolution of raised lettering for all test cubes.....	56
Table 25: Snap fit resolution for all test cubes. Green boxes indicate the offsets that correspond to the best fit between the peg and slots.....	57
Table 26: Gap accuracy machine variability analysis.....	59
Table 27: Hole accuracy machine variability analysis.....	60
Table 28: Thin wall accuracy machine variability analysis	60
Table 29: Linear Accuracy mean differences	73
Table 30: Gap accuracy mean differences	73
Table 31: Hole accuracy mean differences	73
Table 32: Thin wall accuracy mean differences	74

List of Figures

Figure 1: Example air duct where AM can be used to consolidate a multistep, multipart assembly into a single part. [2]	1
Figure 2: SLS process diagram [5].....	3
Figure 3: Previous metrology efforts.....	6
Figure 4: Polymer test cube as-built (left) and disassembled (right) [10]	9
Figure 5: Test cube labels.....	10
Figure 6: Test cube base and surface roughness feature	11
Figure 7: Panel containing linear accuracy, cylindricity, dome, and cone features	12
Figure 8: Panel containing hole resolution and accuracy as a function of wall thickness feature	12
Figure 9: Panel containing gap accuracy as a function of wall thickness feature	12
Figure 10: Panel containing thin wall, hinge, thin rod resolution, and thick rod accuracy features	13
Figure 11: Panel containing snap fit and lettering features (embossed lettering on reverse side).....	13
Figure 12: 3D Systems Sinterstation HiQ+HS platform [11]	16
Figure 13: Build chamber axis description. The recoating roller moves along the X-direction when depositing new layers of powder.	17
Figure 14: Convention used to describe Interior and Exterior locations within the build chamber.....	20
Figure 15: Image generated from optical surface profiler	24

Figure 16: Linear accuracy test part (left) and recommended caliper placement (right) .	25
Figure 17: Gap accuracy test part. Measurements are taken at each of the four locations listed for each wall thickness.	25
Figure 18: Hole diameter as a function of wall thickness test part (left) and example digitally processed measurement scan (right).....	26
Figure 19: Thin wall test part, with measurement locations indicated.....	27
Figure 20: Thin rod pass/fail criteria	27
Figure 21: Hinge test part. The top hinge has a shaft offset of 1.0mm and the bottom hinge has a shaft offset of 0.6mm.	28
Figure 22: Snap fit test part, with labels indicating the pegs and slots	29
Figure 23: Surface roughness as a function of angle relative to build plane.....	34
Figure 24: Average surface roughness as a function of build angle for all test cubes	35
Figure 25: Observed stair-stepping at different angles relative to the build chamber.....	36
Figure 26: Linear accuracy test part	37
Figure 27: Linear accuracy trend for all test cubes	38
Figure 28: Gap accuracy as a function of wall thickness test part	40
Figure 29: 1.4mm gap accuracy as a function of wall thickness for all test cubes	40
Figure 30: Hole diameter as a function of wall thickness test part	42
Figure 31: 2.6mm hole accuracy as a function of wall thickness for all test cubes	43
Figure 32: Thin wall test part	46
Figure 33: Thin wall accuracy for all test cubes. Measurements were taken in the middle of the wall.	47

Figure 34: Thin rod test part.....	51
Figure 35: Hinge test part.....	53
Figure 36: Raised and embossed lettering test part.....	55
Figure 37: Mechanical snap fit test part.....	57
Figure 38: Convention used for analyzing snap fits.....	58
Figure 39: Web tool layout.....	63
Figure 40: Interactive web tool filtered to display the results for all cubes built in GF PA 12 and in the XY orientation.....	65
Figure 41: Interactive chart tool filtered to display results for all cubes built in GF PA 12 and in the XZ orientation.....	65

Chapter 1 Introduction

1.1 Motivation

Additive manufacturing offers a number of advantages over traditional subtractive machining techniques. AM technologies can expand the design space, allowing previously unachievable geometric complexity and yielding vastly improved part performance. For instance, aircraft manufacturers use AM to make innovative aircraft ductwork, which provides significant weight savings and reduces assembly time by consolidating parts [1]. One such example is shown in Figure 1, where a 16 part assembly is reduced to a single part through implementing AM [2]. AM can also improve sustainability of manufactured products, reduce time to market, and eliminate tooling costs that would be required for other manufacturing processes [3]. One factor preventing widespread adoption of AM in manufacturing is that designers have limited knowledge of the geometric capabilities and limitations of each process.

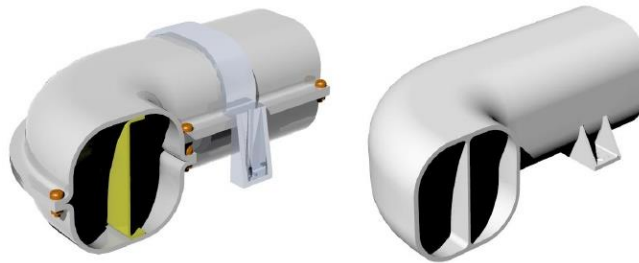


Figure 1: Example air duct where AM can be used to consolidate a multistep, multipart assembly into a single part. [2]

Metrology strategies are needed to characterize each AM process so that designers can compile detailed, statistical knowledge of the geometric resolution and accuracy for different features of interest. An uncharacterized process can lead to mistakes that require

iteration before the final design intent is reached, thereby diminishing the benefits of AM. A comprehensive metrology study can help designers reduce the number of design iterations and realize parts as they were originally intended in a more timely fashion. A critical component of a metrology study is a test part that incorporates the features of interest to the designer.

In addition to supporting statistical characterization of an AM process, a standard metrology test part can also help manufacturers monitor machine performance over time. The tuning parameters used on a machine can affect part quality, and these parameters often vary from machine to machine. Machine operators can use test parts to evaluate machine performance compared with an “average” well-tuned machine. The same test parts can also be used for the purpose of calibrating both new and existing machines.

1.2 SLS Process Overview

Selective laser sintering (SLS) is a process of interest for industrial applications because it can be used to create functional, end-use parts that have a high degree of geometric complexity. However, many designers are unaware of the capabilities and limitations associated with the process. The benefits offered by additive manufacturing are hindered when a proper design for additive manufacturing (DFAM) knowledge base is not established. Despite the availability of several test parts that can be built in SLS, there are no publicly available metrology studies that provide a statistically significant, comprehensive overview of the geometric capabilities of SLS.

Selective laser sintering is the AM process by which powder is fused selectively with a laser-based energy source. A thin layer of polymer powder is spread across a heated build

platform. A CO₂ laser then scans the cross section of the part to fuse the powder, and another layer of powder is deposited above it. This process is repeated until the part is completed. In order to alleviate residual stresses caused by the subsequent heating and cooling associated with the layering step, the entire build chamber is heated to a temperature that is just above the glass transition (T_g) temperature of the material [4]. Additionally, fabricating the part in a powder-filled build chamber allows features in SLS to be self-supporting, meaning support structures are not required for bridges and overhangs.

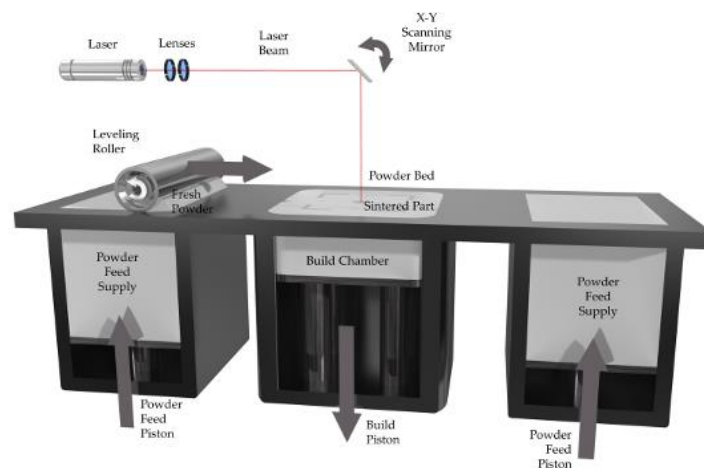


Figure 2: SLS process diagram [5]

1.3 Requirements for Metrology Test Part

In order to realize the benefits of SLS, a greater understanding of the process is needed. Test parts can be used in a metrology study to characterize the SLS process. These test parts must be compact so they can easily fit within SLS builds. By occupying a small volume, many copies of the test part can be created. It is important to build as many copies as possible to add statistical robustness to the metrology study.

Additive manufacturing (AM) encompasses many different processes, each with unique capabilities and limitations [3]. Test parts in an AM metrology study must be process-specific in order to fully assess the nuances of each technology. They must also contain features of interest to a designer. The features included should highlight the specific capabilities of SLS that can be leveraged in AM designs. The test part should reflect the geometric complexity achievable by SLS due to the lack of need for support structures.

Lastly, the greatest benefit of the test part is attained by maximizing the feature density. Feature density is defined as the total number of measureable feature instances per unit volume of the test part. A high feature density corresponds to more information obtained from each copy of the test part. Feature density is a measure of how efficiently the features are packed within a test part. This is important when creating many copies because inefficient designs would lead to a higher cost.

1.4 Previous Work

Figure 3 illustrates several test parts from previous efforts to characterize AM processes. A 2004 Mahesh study sought to design a standardized AM test part. The part was built using four different AM processes (SLA, SLS, LOM, FDM) with widely varying results [6]. While this part can be useful for comparing the relative strengths and weaknesses of different AM methods, it fails to capture specific nuances inherent to each process.

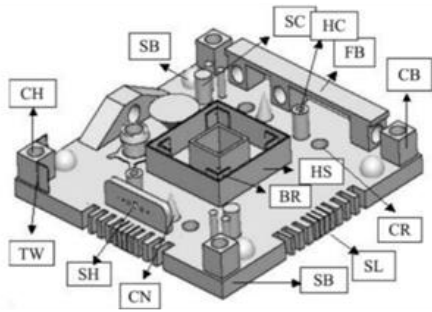
A 2005 Castillo study proposed a test part for selective laser melting (SLM) to be used for comparing the behavior of different metal powders [7]. The large volume of the test

part and limited number of features contributed to a low feature density (number of feature instances per unit volume).

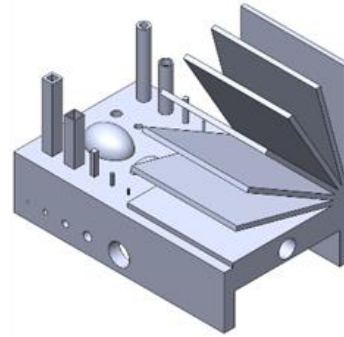
A study by Govett et al. took a different approach when performing a geometric characterization of the SLS process. Instead of using a single test part with integrated features, individual parts were made for each feature [8]. This allowed the features to be studied exhaustively, capturing both the resolution and accuracy of the process. Holes, thin rods, thin walls, gaps, hole proximity to wall, shaft clearance, lettering, and gears were all considered in the study. The results were presented as a series of color-coded charts for resolution and trend graphs for accuracy, allowing a designer to quickly understand the effects. However, such a comprehensive study came at the cost of a large build volume required to build each of the parts. The build volume required to complete a single round of these parts totaled approximately 5,000 cm³, which was an order of magnitude larger than other metrology efforts. The required build volume limited the number of test part copies that could be produced. For this reason, only two replicates were used in the study. The greatest weakness of this study was that the large build volume detracted from the statistical significance of the results.

Finally, another attempt at a standardized AM test part was made by Moylan et al. in 2014. The proposed test artifact occupies a relatively small build volume (100x100x17mm) while incorporating a variety of features [9]. However, this part is not process-specific and fails to fully utilize the capabilities of polymer PBF, namely the lack of a need for support structures.

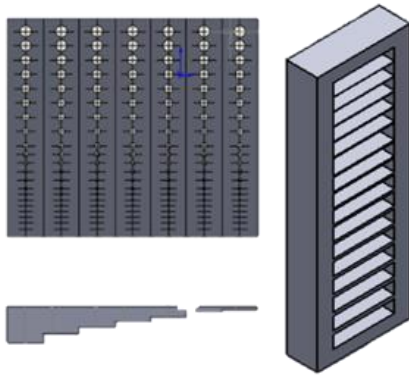
These studies highlight the need for a compact test part that encompasses a wide array of features that can be used in polymer powder bed fusion. A test part designed for SLS can raise the feature density while maintaining a compact profile.



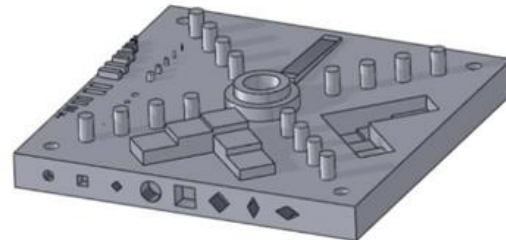
Mahesh (2004)



Castillo (2005)



Govett (2012)



Moylan (2014)

Figure 3: Previous metrology efforts

1.5 Research Goals

The goal of this thesis is to present a test part specifically designed for polymer selective laser sintering and a corresponding metrology strategy. The test part can be used to statistically characterize the SLS process as well as help manufacturers monitor machine performance over time.

This research also seeks to implement the proposed metrology strategy and establish a set of design for additive manufacturing guidelines for SLS. The guidelines can help designers reduce the number of design iterations and realize parts as they were originally intended in a more timely fashion. They can also be used by novice designers that do not have previous experience with the SLS process.

Another objective of this research is to make the results accessible to the public through an online web tool. By presenting both high and low level guidelines, the tool can be used by any designer, regardless of prior AM knowledge. The tool will also allow experienced designers to interactively interrogate the data to uncover trends in greater detail.

Chapter 2 Design of a Test Part

2.1 Introduction

The requirements outlined in Section 1.3 form the basis for a polymer PBF test part. Compactness is one of the most important aspects because it allows the test part to be replicated efficiently. The proposed test part is designed for polymer PBF to be used in a metrology study. It includes various features of interest to a designer and is intended to capture both the resolution and accuracy of the SLS process.

2.2 SLS Test Part Design

In order to provide statistically significant information on the geometric capabilities of the SLS process, many copies of the test part are required. The SLS process allows parts to be stacked within the build entire build volume, allowing open spaces to be utilized. It is necessary for the test part to be compact so that it can be placed within the open spaces of existing production builds. The dimensions of the test part are limited to a cube measuring two inches on each side, allowing it to be easily placed into existing builds. All test part copies are built by Stratasys Direct Manufacturing (Austin, TX, USA) as part of production builds so that the metrology study reflects the capabilities of production-quality builds.

The focus of this study is to characterize the geometric capabilities of polymer selective laser sintering (SLS) using a test part that is both compact and comprehensive. The test part, shown in Figure 4, consists of five panels connected to a common base through small tabs. Each panel contains different geometric features and can be removed from the base for measurement. When built, the test piece occupies a cube measuring two inches along

each side. By taking advantage of the self-supporting nature of the SLS powder bed, a high feature density was achieved by closely grouping the features.

Combining aspects found in previous test parts (Section 1.2), this design features a comprehensive variety of features in a compact cube. The part is built as a single unit, similar to the parts proposed by Mahesh, Castillo, and Moylan. The detachable panels are analogous to the individual feature test parts used in the Govett et al. study. By making use of existing knowledge of the SLS process, the resulting test part is both compact and comprehensive. Other AM processes, such as fused deposition modeling (FDM) would be unable to build this test part due to the many bridges and overhangs.

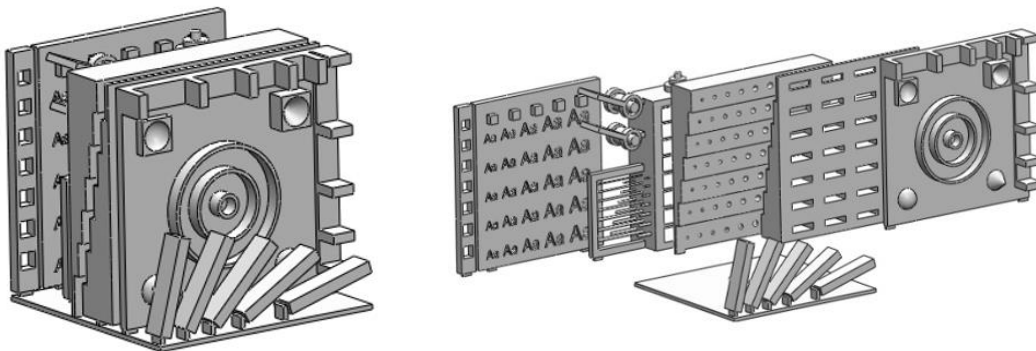


Figure 4: Polymer test cube as-built (left) and disassembled (right) [10]

Small protruded features beneath the base can be added to individually identify each cube, as in Figure 5. Here, the labeled axes of the protrusion correspond to the plane in which the base was aligned within the build chamber. The “e” marking denotes that the cube is to be built along the exterior, or perimeter, of the build chamber. Further discussion of this convention is covered in Chapter 3.

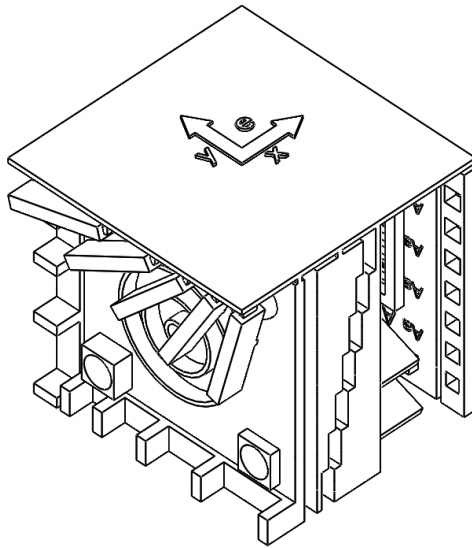


Figure 5: Test cube labels

In an effort to design a test part that is both comprehensive and compact, the sizing of each feature is especially important. Drawing on the results of the 2012 Seepersad SLS characterization study, the feature sizes are designed to range between those that are large enough to be built reliably and those that are likely too small to be resolved [8].

2.3 Features Considered

Table 1 provides a summary of the features included in the test cube as well as the range of sizes investigated. The “Increment” column denotes the incremental increase along the dimension of interest. For example, hole diameters are varied between 0.8 and 2.6mm in 0.2mm increments. In this case, hole diameters of 0.8, 1.0, 1.2, 1.4, 1.6, 1.8, 2.0, 2.2, 2.4, and 2.6mm are incorporated into each wall thickness. Figures 6-11 show each panel of the test cube with dimensions corresponding to each feature. The range of feature sizes was chosen based on the results of previous studies. At the lower end of the range, features are likely too small to be built. At the upper end, features are large enough to

almost certainly resolve. In this way, both accuracy and resolution of the process can be determined.

Table 1: Polymer test cube feature ranges [10]

Feature	Feature Ranges	Increment
Holes	0.8-2.60mm diameter	0.2mm
	1.0-10.0mm wall thickness	1.5mm
Thin rods	0.3-0.9mm diameter	0.1mm
Thin walls	0.2-0.8mm	0.1mm
Gaps	1.4-2.0mm gaps	0.2mm
	1.0-10.0mm wall thickness	1.5mm
Cylinders	2.0-8.0mm diameter	3.0mm
Hollow cylinders	5.0-25mm diameter	10.0mm
Domes	6.0mm diameter	-
Cones	6.0mm diameter	-
	5.2mm height	-
Linear accuracy	5.0-12.5mm	2.5mm
Surface roughness	0°-90°	15°
Hinges	0.6mm and 1.0mm shaft clearances	-
Lettering	10-18pt font	2pt
	0.5-2.5mm emboss/raised depth	0.5mm
Snap Fits	-0.5-0.25mm offsets	0.05mm

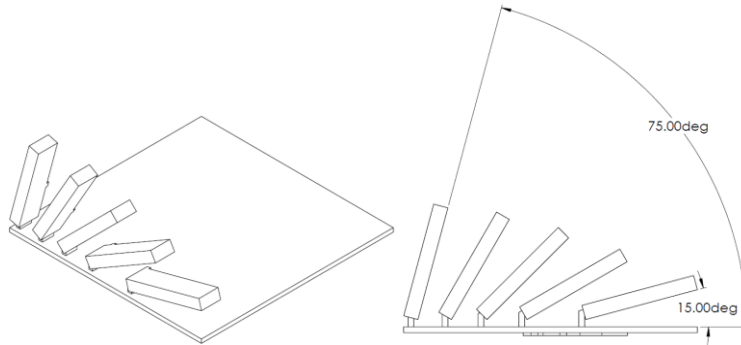


Figure 6: Test cube base and surface roughness feature

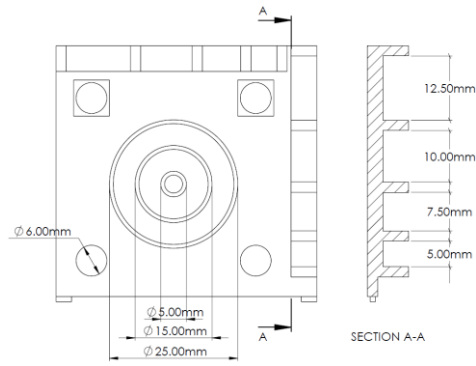


Figure 7: Panel containing linear accuracy, cylindricity, dome, and cone features

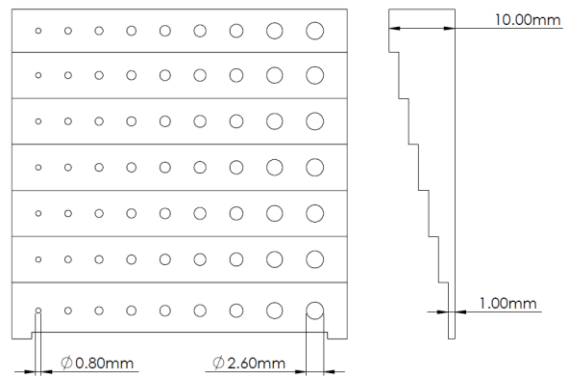


Figure 8: Panel containing hole resolution and accuracy as a function of wall thickness feature

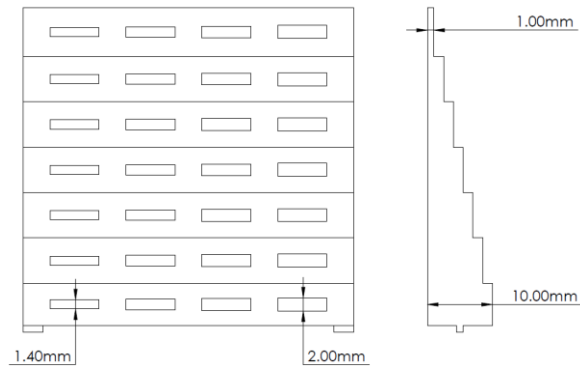


Figure 9: Panel containing gap accuracy as a function of wall thickness feature

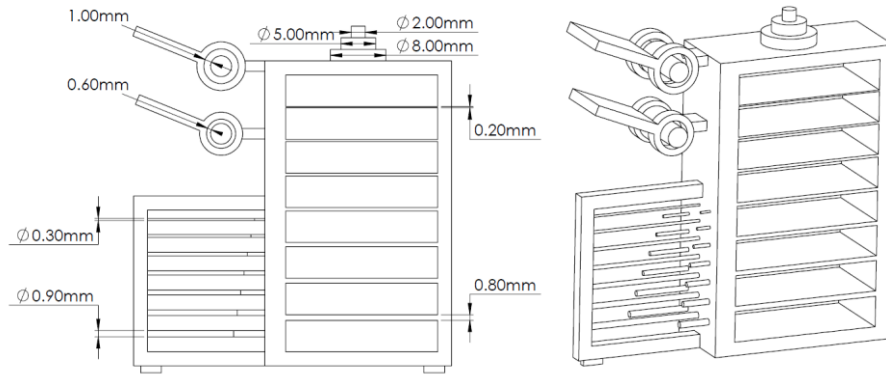


Figure 10: Panel containing thin wall, hinge, thin rod resolution, and thick rod accuracy features

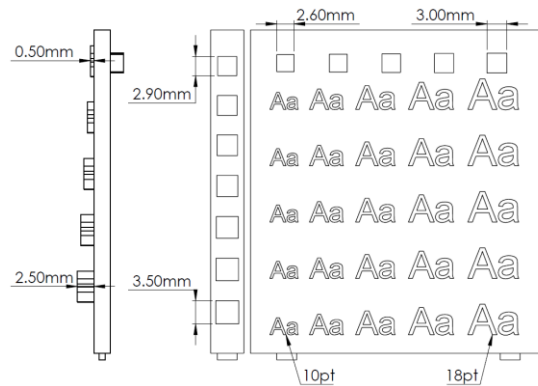


Figure 11: Panel containing snap fit and lettering features (embossed lettering on reverse side)

As a means of comparison, the features included in previous test parts have been tabulated below along with the size of each part. The number of instances of each particular feature incorporated into the test part is shown in parentheses beside the feature description. Feature density is then calculated by dividing the total number of instances by the bounding volume of the part. Here it can be seen that the proposed part in this study not only occupies the smallest build volume, but also has the highest feature density.

Table 2: Comparison of different test parts, including dimensions and feature density [10]

	Mahesh (2004)		Castillo (2005)		Govett (2012)		Moylan (2014)		Proposed Part	
Bounding Dimensions	170x170x20mm		60x81x100mm		-		~100x100x17mm		51x51x51mm	
Bounding Volume	578 cm ³		486 cm ³		~5,000 cm ³		~170 cm ³		131 cm ³	
Features Considered	Holes	(14)	Holes	(15)	Holes	(147)	Holes	(10)	Holes	(63)
(Number of instances)	Thin rods	(6)	Thin rods	(5)	Thin rods	(15)	Thin rods	(5)	Thin rods	(21)
	Thin walls	(2)	Thin walls	(3)	Thin walls	(92)	Cylinders	(16)	Thin walls	(7)
	Gaps	(22)	Domes	(2)	Gaps	(154)	Linear accuracy	(10)	Gap	(28)
	Hollow Cylinders	(2)	Square rods	(5)	Hole proximity to wall	(73)	Rectangular boss	(10)	Cylinders	(3)
	Domes	(4)	Bridge	(1)	Shaft clearance	(104)	Surface roughness	(1)	Hollow cylinders	(3)
	Cones	(2)	Warping	(1)	Lettering	(608)	Flatness	(1)	Domes	(2)
	Square rods	(8)	Overhang angles	(7)	Gears	(6)	Build axis alignment	(1)	Cones	(2)
	Bridge	(2)					Lateral features of varied cross-section	(8)	Linear accuracy	(8)
	Hollow squares	(2)							Surface roughness	(7)
	Flatness	(1)							Hinges	(2)
	Straightness	(1)							Lettering	(50)
	Brackets	(4)							Snap Fits	(5)
Feature Density (instances/cm³)	0.12		0.08		0.24		0.36		1.53	

Chapter 3 Overview of Metrology Study

3.1 Introduction

The test part described in Chapter 2 can be used in a factorial-style study to characterize the SLS process. Four factors in particular can affect the accuracy and resolution of a variety of features in a PBF process and can be easily modified and specified by the designer. The four factors are material choice, orientation of the test part within the build chamber, location of the test part within the build chamber, and machine identity. By varying each of these factors, a factorial experiment can be conducted. Other process parameters such as scan speed, laser power, and scan spacing are not considered because these parameters are typically inaccessible to the customer. The results represent feature capabilities for commercially tuned machines in production builds.

When planning a metrology study, it is important to build multiple copies of the test part under different conditions to fully characterize a PBF machine or process. For each unique material, orientation, and location combination, five replicates are built on a single machine. Table 3 shows the experimental design, where each box represents a different copy of the test cube. This study requires 90 replicates of the test part to be built and analyzed.

Table 3: Metrology study experiment design.

	Orientation	Location	Replicates			
FR PA 11	XY	I				
	XY	E				
	XZ	I				
	XZ	E				
	YZ	I				
	YZ	E				
PA 12	XY	I				
	XY	E				
	XZ	I				
	XZ	E				
	YZ	I				
	YZ	E				
GF PA 12	XY	I				
	XY	E				
	XZ	I				
	XZ	E				
	YZ	I				
	YZ	E				

All test parts were built by Stratasys Direct Manufacturing on 3D Systems Sinterstation 2500 Plus and 3D Systems Sinterstation HiQ+HS machines featuring Integra multizone heater upgrades. A similar system is shown in Figure 12 below. The machines were maintained by Stratasys and tuned to production level specifications.



Figure 12: 3D Systems Sinterstation HiQ+HS platform [11]

Figure 13 describes the convention used to define the axes of the build chamber. Layers are deposited across the XY plane and stacked along the Z-axis during a build.

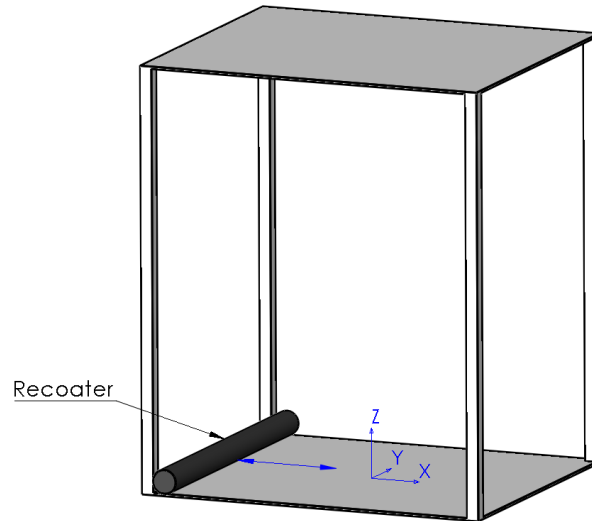


Figure 13: Build chamber axis description. The recoating roller moves along the X-direction when depositing new layers of powder.

3.2 Material

Material selection is important for polymer PBF. It affects not only the mechanical and thermal properties of resulting parts, but also sintering-related properties such as shrinkage, stress relaxation, oversintering, and surface roughness [4] [12] [13].

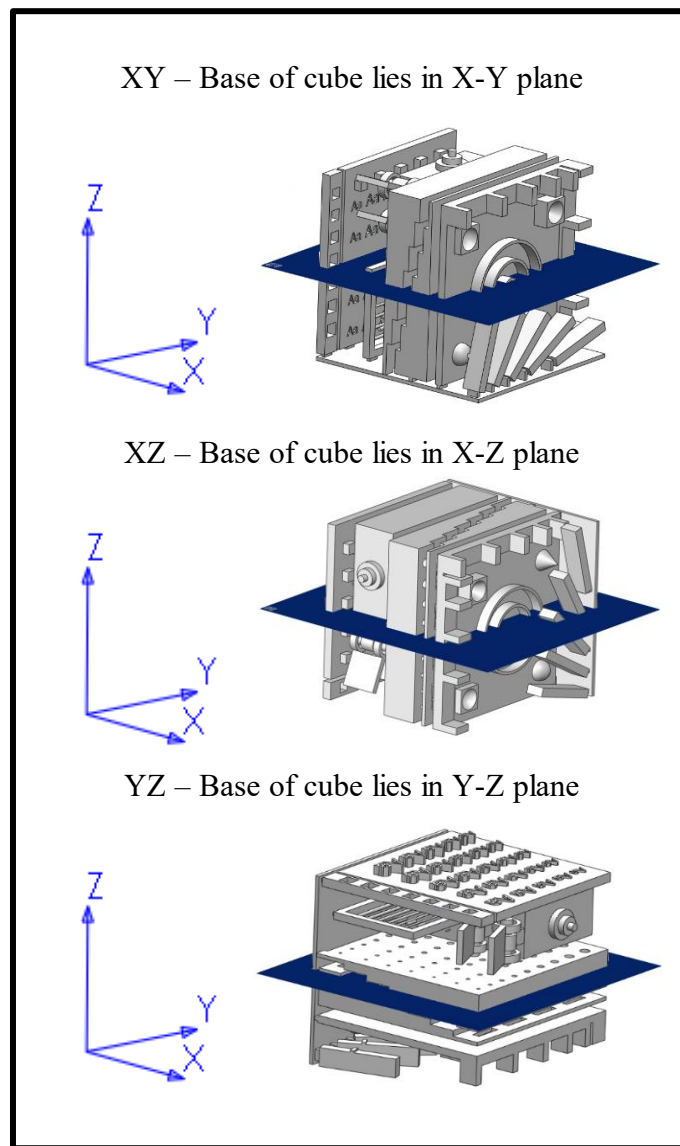
Three materials are being considered in this study. The first is a fire retardant blend of polyamide nylon 11 (FR PA 11). The tensile strength of fire retardant nylon 11 is slightly lower than unmodified or “neat” nylon 11, but it offers superior flame resistance. For this reason, it can be used for electrical component housings, insulations, and aircraft trim [14]. The second material in this study is an unmodified blend of polyamide nylon 12 (PA 12). PA 12 is one of the most widely used polymers in laser sintering, noted for having a larger processing window than PA 11 [15]. The third material studied is a glass composite blend

of polyamide 12 (GF PA 12). The composite consists of nylon 12 powder blended with glass beads, which can lead to better mechanical properties.

3.3 Orientation within Build Chamber

Similar to other AM processes, polymer PBF is prone to having anisotropic properties in finished parts [16]. Cooke et al. showed that parts tend to be weaker out of the plane of the layers (Z-axis), while fairly isotropic in-plane [17]. This weakness can be attributed to imperfect bonding between successive layers. In-plane homogeneity can be further improved through machine parameters such as laser cross hatching, but with little effect on out-of-plane properties. Geometric accuracy and resolution can also be affected by the orientation within the build chamber. The laser scans across the XY plane of the build chamber at each layer. Consequently, the accuracy and resolution of features that lie along this plane are greatly influenced by the diameter of the laser spot. Features that are oriented through the depth of the build chamber (Z-axis), however, have a greater dependence on the layer thickness for accuracy and resolution. The orientation in which features are positioned can therefore dramatically affect the resulting feature quality [18]. The test part can be fabricated in three different orientations corresponding to the major axes of the build chamber to assess orientation affects. Table 4 shows the convention used for part orientation.

Table 4: Convention used for describing orientation of test cubes within the build chamber



3.4 Location within Build Chamber

Powder bed fusion for polymers requires a heated build chamber to alleviate residual stresses within the parts. Uneven heating of the build chamber can lead to thermal gradients across the powder surface. This variation within the build environment can have

unexpected consequences such as varying accuracy and strength, depending on where the parts were built in the build chamber. Convection channels and cooling from the build chamber walls can cause thermal gradients across the part bed. The corners of the chamber tend to be cooler than the center, and parts located there tend to be less ductile with a higher degree of warping [19].

Two different locations within the build chamber are used in this study. Exterior (E) test cubes are built along the perimeter of the build chamber, while Interior (I) cubes are placed near the center. This convention is depicted in Figure 14, where the blue box represents the Exterior region, and the white box represents the Interior region. Only locations along the XY build plane are taken into account. Although conduction from previously sintered layers may contribute to thermal gradients, locations along the build depth are not considered within the scope of this study.

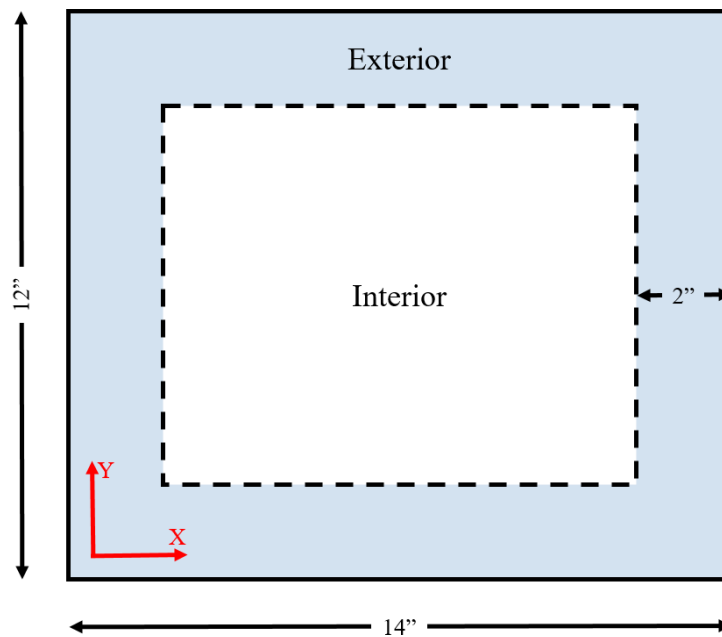


Figure 14: Convention used to describe Interior and Exterior locations within the build chamber

3.5 Machine Variability

Machine identity can also impact part quality. Without considering specific machine tuning parameters, building the same part on different machines can yield different results due to differing machine calibration, repair and maintenance schedules, and other factors. Multiple replicates built on different machines allows machine variation to be taken into account [12].

In order to assess machine variability, three replicates at each material, orientation, and location combination were built on a second machine and compared with the five replicates built on the first machine. The updated experimental design to include machine variability is shown in Table 5. In total, 144 copies of the cube must be built to complete the test matrix.

It is worth noting that machine variation in this study is taken on a per-material basis. For example, all FR PA 11 replicates under “Machine 1” were built in the same machine, but a different machine was used to produce each of the PA 12 “Machine 1” copies. The test parts were built in production builds conducted by Stratasys Direct Manufacturing. As a service bureau that seeks to run a high volume of builds, machines are typically dedicated to specific materials to reduce changeover time and powder contamination.

Table 5: Experiment design including machine variability

	Orientation	Location	Machine 1				Machine 2		
FR PA 11	XY	I							
	XY	E							
	XZ	I							
	XZ	E							
	YZ	I							
	YZ	E							
PA 12	XY	I							
	XY	E							
	XZ	I							
	XZ	E							
	YZ	I							
	YZ	E							
GF PA 12	XY	I							
	XY	E							
	XZ	I							
	XZ	E							
	YZ	I							
	YZ	E							

Chapter 4 Measurement Procedure

4.1 Introduction

Several measurement methods were implemented to gather geometric information from the test cubes. When carrying out the metrology study, it was important to pair the feature type with an appropriate measurement technique. For the features that required the use of calipers, the measurement system was validated using a Gage R&R study.

4.2 Measurement Techniques

4.2.1 Surface Roughness

Surface roughness is typically reported as the average height of a surface along a single dimension. Average roughness (R_a) and root-mean-square roughness (R_q) values are typically used. R_a is calculated by taking a straight average of the surface data, and R_q is calculated by taking the root-mean-square of the height values. Surface roughness is most commonly determined using mechanical profilometers, which work by moving a sensor across the dimension of interest and measuring the deviation from the mean surface height. Mechanical profilometers require physical contact with the part to generate measurement data. In practice, mechanical methods are unreliable in measuring the roughness of laser sintered polymer parts. As the sensor sweeps the part, the material is deformed at the contact interface because of its softness. Optical methods, then, are the preferred measurement technique for surface roughness.

Surface roughness is measured using a Zeta 3D optical profiler. While mechanical profilometers are limited to a single dimension, the optical profiler allows surface roughness to be calculated across a two dimensional plane. Instead of linear roughness (R_a

and R_q) generated through mechanical techniques, the optical profiler outputs area roughness (S_a and S_q). Using a high precision camera, the profiler generates a 3D image of the part surface (Figure 15), and the roughness is calculated according to equations 4.2.1.1 and 4.2.1.2. S_a and S_q can be interpreted as the average R_a and R_q measurements across the scanned surface. The field of view for the camera is 3.1mm by 1.2mm.

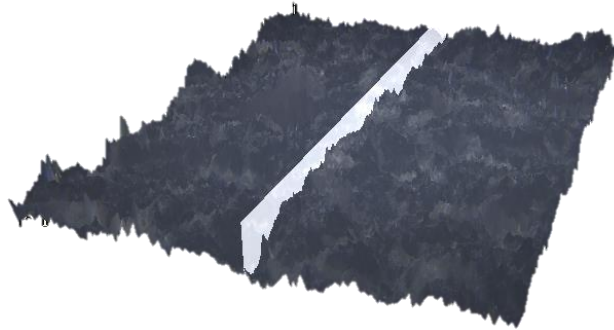


Figure 15: Image generated from optical surface profiler

$$S_a = \iint_a |Z(x, y)| dx dy \quad (4.2.1.1)$$

$$S_q = \sqrt{\iint_a (Z(x, y))^2 dx dy} \quad (4.2.1.2)$$

4.2.2 Linear Accuracy

Linear accuracy was measured with iGaging digital calipers (0.01mm resolution). Figure 16 shows the linear accuracy test part and how it was measured. Using the upper jaws of the calipers, each gap distance was reported. In order to ensure measurement consistency, measurements were taken from the base of each gap as depicted in the right image of Figure 16. Three measurements were recorded for each gap and averaged.

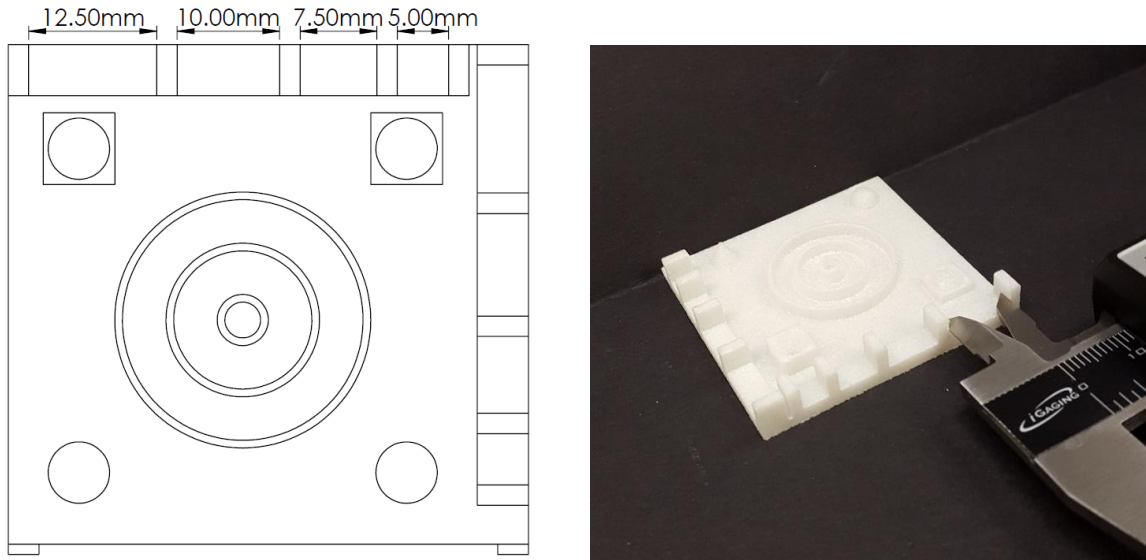


Figure 16: Linear accuracy test part (left) and recommended caliper placement (right)

4.2.3 Gap Accuracy as a Function of Wall Thickness

iGaging digital calipers (0.01mm resolution) were used to measure the gaps at each wall thickness. For the thinner walls, extra care was given not to deform the material while taking measurements. Three measurements were recorded and averaged.

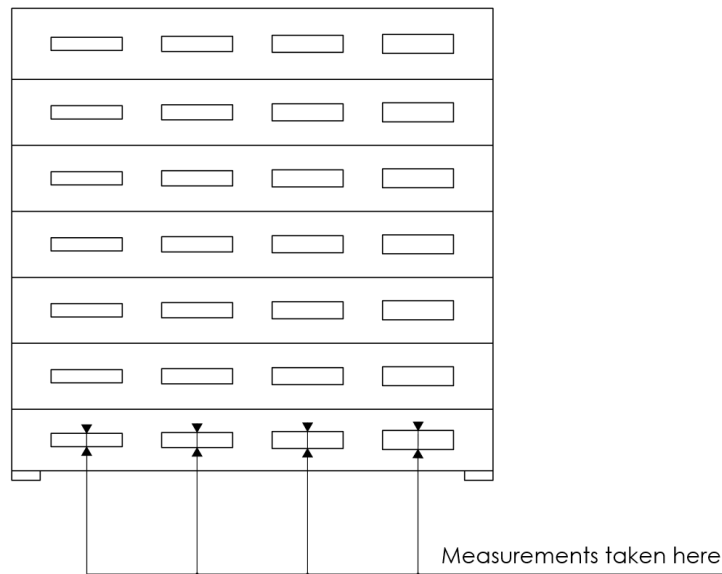


Figure 17: Gap accuracy test part. Measurements are taken at each of the four locations listed for each wall thickness.

4.2.4 Hole Diameter as a Function of Wall Thickness

Hole diameter was measured using an optical flatbed scanner and processed in MATLAB. As shown in Figure 18, the scanned image was converted to black and white. The calibration square is used to individually scale each image according to a 1cm by 1cm square that is placed on the scanner next to the part. The MATLAB code determines the area of each hole by counting the white space and uses it to calculate the diameter. It should be noted that eccentricity of the holes are not taken into account, so average diameter is reported. This measurement system was verified against pin gages.

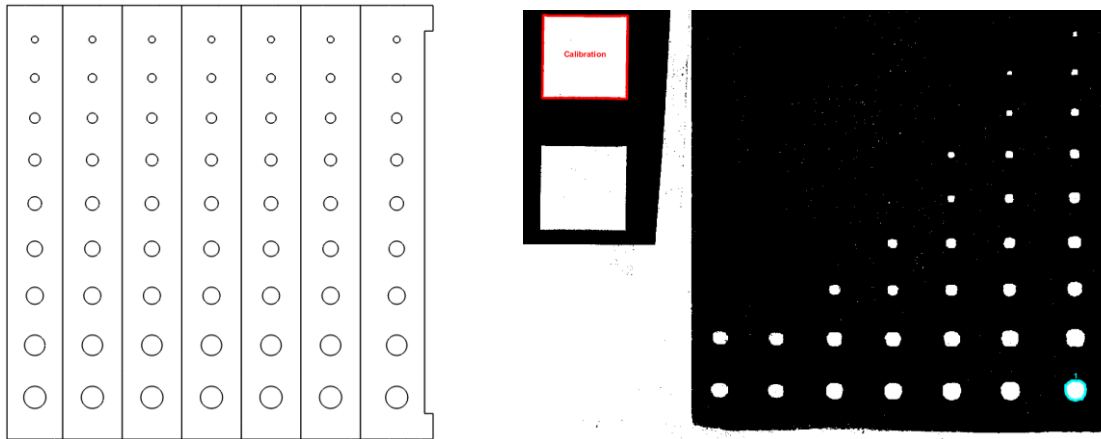


Figure 18: Hole diameter as a function of wall thickness test part (left) and example digitally processed measurement scan (right)

4.2.5 Thin Walls

The thin walls were measured using iGaging digital calipers (0.01mm resolution). Two measurements of each wall were taken - one at the edge and one in the center, noted in Figure 19 below. Three measurements at each location were recorded and averaged. If the wall was warped due to being too thin or if the wall was too thin to be built, it was marked as a “Fail.”

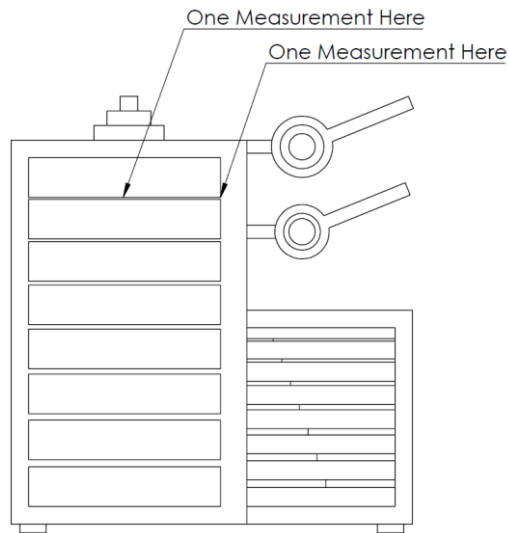


Figure 19: Thin wall test part, with measurement locations indicated

4.2.6 Thin Rods

The thin rods were documented using pass/fail criteria according to whether the feature built or not. If the rod was successfully built, it was marked as a “Pass.” If the feature did not resolve, it was recorded as “Fail.” Figure 20 shows an example part with passed and failed rods marked. Diameter measurements were not taken into account, so only resolution data was reported.

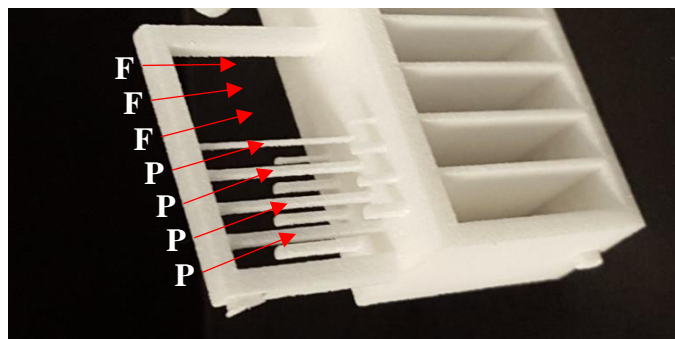


Figure 20: Thin rod pass/fail criteria

4.2.7 Hinges

Hinges were also rated with pass/fail criteria. The hinges were tested by checking if the panel moved freely after gently deflecting it, and “Pass” or “Fail” was reported depending on the result. The hinge test part can be seen in Figure 21 with the top hinge corresponding to the larger shaft offset.

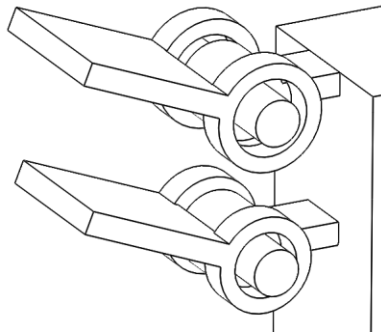





Figure 21: Hinge test part. The top hinge has a shaft offset of 1.0mm and the bottom hinge has a shaft offset of 0.6mm.

4.2.8 Lettering

Lettering was evaluated on a Pass/Fail/Intermediate scale. “Pass” was given to letters that were clearly legible with no defects. “Intermediate” was given to letters that were legible, but had minor defects. “Fail” was given to letters that were not legible or had substantial defects. Examples of each rating are shown in Table 6.

Table 6: Convention used to determine resolution of lettering features

		
Pass	Intermediate	Fail

4.2.9 Snap Fits

For the snap fits, the convention in Figure 22 was used to correlate which peg fits snugly in each slot, starting with the largest slot and moving to the smallest. This ensured that the pegs would not deform during testing. As soon as the slot provided a tight fit with the peg, it was recorded and the next peg was tested.

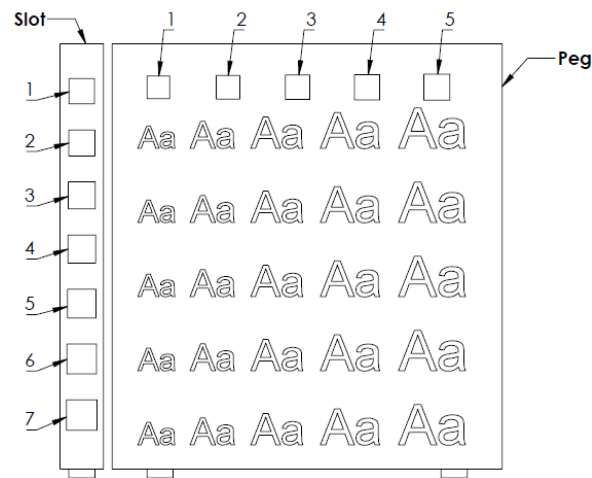


Figure 22: Snap fit test part, with labels indicating the pegs and slots

4.3 Gage Repeatability and Reproducibility (Gage R&R)

Gage R&R is the statistical method used to quantify the variation introduced by the measurement system, including the measurement device and operators taking the measurements. The value reported indicates the percentage of variation that can be attributed to the measurement system. Gage R&R works by measuring the total part variation across multiple parts, trials, and operators. Each repeated measurement of a part is called a trial, and the operators are the individuals collecting measurements. The total variation is then compared with an estimate of part-to-part variance in order to determine the variance of the measurements. R&R values between 10% and 30% are generally considered acceptable [20]. A Gage R&R study is performed on the caliper measurements,

namely linear accuracy, gap size, and wall thickness. The R&R study uses 12 parts, 3 trials, and 2 operators. The parts are taken from different materials, orientations, and locations within the build chamber. The R&R results are shown in Table 7 below.

Table 7: Gage R&R results for linear accuracy

Feature	R&R (%)
Linear Accuracy	20.21
Gap Size	40.49
Wall Thickness	20.16

Here it can be seen that linear accuracy and wall thickness fall within the acceptable range, but gap size is slightly outside. The high R&R value associated with gap size can be attributed to the fact that the observed part-to-part variation is extremely small, so a larger percentage of variation comes from the measurement system.

Chapter 5 Design Guidelines

5.1 Interpretation of Results

Design guidelines are the means by which process-specific information is relayed to a designer during the design process. For processes that are well-understood, such as machining and injection molding, design guidelines are widely available [21]. Design guidelines must be presented in a way that is easily understood by designers. Previous AM metrology efforts have presented design rules in the form of color-coded charts and trend graphs [8] [22].

A comprehensive metrology study involves collecting large amounts of data in order to characterize a process. The information has limited value, however, if it cannot be succinctly conveyed to a designer. The following sections outline the method used in this thesis to visualize resolution, accuracy, and statistical information in additive manufacturing design guidelines.

5.1.1 Resolution

Resolution can be interpreted as the smallest feature that can be resolved or built. It is expressed here as a color-coded chart for each feature type. Each cell in the chart represents the design of a specific feature (e.g. 2.0mm hole through a 4.0mm thick wall). The color of the cell corresponds to the reliability of the particular feature being built and uses the following convention:

- Green: > 75% of observed instances resolved
- Yellow: Between 25% and 75% of observed instances resolved
- Red: < 25% of observed instances resolved

These colors are only to be used as visual aids. Also included in each cell is the proportion of observed instances resolved. A cell labeled with 0.86, for instance, indicates that 86% of the features for that particular design resolved successfully.

5.1.2 Accuracy

Accuracy can be reported for continuous measurements in the form of a plot. Each of the plots in this chapter consist of two lines. The red line corresponds to the “nominal” dimension specified by the CAD model. The blue line is generated from the measurement results based on the “as-built” features. The error bars at each data point represent the 95% confidence intervals associated with the measurements. The plots presented below are the result of averaging all data for a given feature across orientations, build locations, and materials. To specify one or more of the inputs (material, orientation, location within build chamber), please refer to the interactive web tool described in Chapter 6 of this thesis.

5.1.3 Significant Effects

In order to identify which input parameters have a statistically significant effect on part accuracy, an analysis of variance (ANOVA) test was conducted. The output of the test specifies which factors are significant at a five percent significance level ($\alpha = 0.05$). As a designer, these factors should be considered when creating a part to be manufactured using selective laser sintering. In the tables for significant effects, abbreviations are used to represent each significant factor. Table 8 shows how the abbreviations are interpreted.

Table 8: Interpretation of significant effects tables

Significant Effects	
M	Material
O	Orientation
L	Location
M*O	Material and Orientation Interaction Effect
M*L	Material and Location Interaction Effect
O*L	Orientation and Location Interaction Effect

5.1.4 Mean Differences

After performing the ANOVA test, a multiple comparisons test was conducted to quantify the effect of each significant factor on the feature of interest. In other words, the ANOVA test tells the designer which factors are significant, and the multiple comparisons test quantifies the effect of the factor on the feature of interest. Presented here are the differences in means for main effects (ignoring interaction effects). The following convention is used to describe mean differences:

- SignificantFactor1 – SignificantFactor2
- A negative mean difference indicates the mean of SignificantFactor1 was smaller than SignificantFactor2

An example on how significant effects are displayed to the designer is shown in Table 9.

Table 9: Significant effects visualization example

Thin Wall	
0.2 mm	
XY-YZ	-0.14

In this case – the 0.2mm thin wall – the mean difference between the XY and YZ orientations is -0.14mm, meaning YZ walls are generally 0.14mm thicker than XY walls.

5.2 Design Guidelines by Feature Type

The design guidelines are structured to encompass varying levels of detail, starting at a high level overview and increasing in specificity. Depending on the application, the designer may want more or less information from the guidelines. The high level overview provides qualitative insight into AM best practices, while the trends and explanations give quantitative values for the different features.

5.2.1 Surface Roughness

Surface roughness is related to texture. Parts with a low surface roughness feel smooth, while those with a high surface roughness feel rough. For angles between 15 and 75 degrees relative to the build plane, the small tabs are removed and measured (Figure 23). The base is used for the zero degree measurement, and a vertical panel on the test cube is used for the 90 degree measurement.

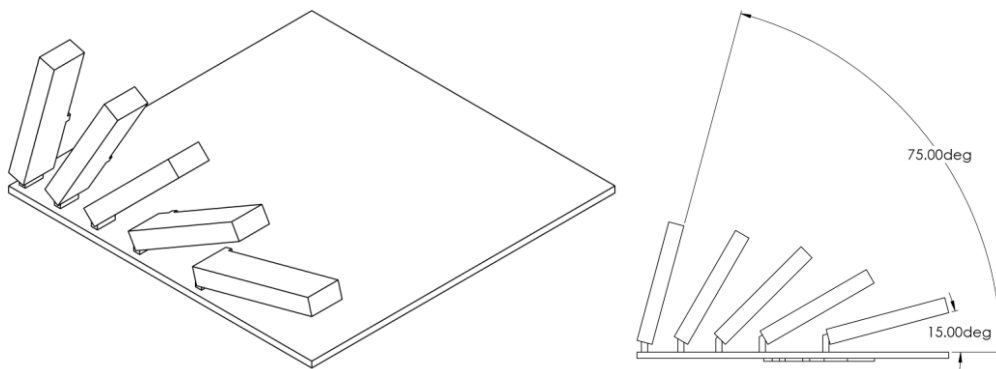


Figure 23: Surface roughness as a function of angle relative to build plane

General Guidelines

- Surface roughness is smallest parallel to the build plane
- The greatest roughness occurs at 15 degrees relative to the build plane
- Average surface roughness tends to vary between 20 and 35 μm

Results

The average surface roughness results from all test cubes are shown in Figure 24. The surface roughness is smallest at an angle of zero degrees relative to the build plane. The maximum roughness occurs at 15 degrees then decreases at all subsequent angles. Despite the decreasing trend, the roughness is still reaches its minimum value at zero degrees. FR PA 11 is rougher than both PA 12 and GF PA 12, which have similar values of roughness. There does not appear to be a strong correlation between location within the build chamber and surface roughness.

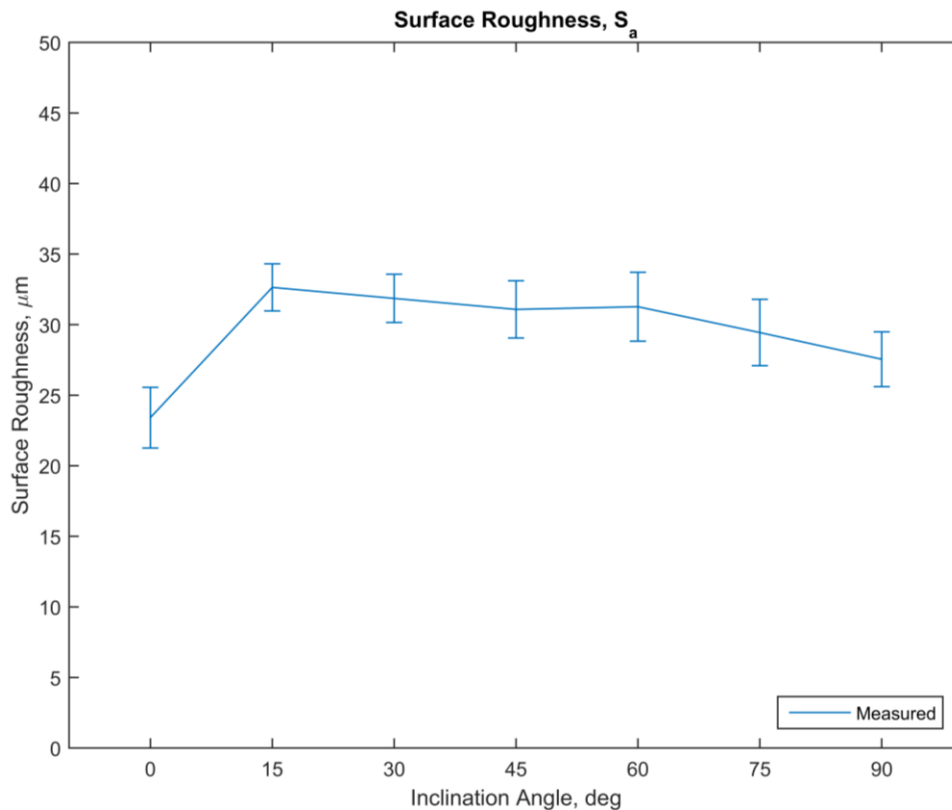


Figure 24: Average surface roughness as a function of build angle for all test cubes

Explanation

The driving factor behind surface roughness is the layering effect that occurs in additively manufactured parts. Owing to the fact that parts are created layer-by-layer, stair steps are formed at angles that are not orthogonal to the build axes. Figure 25 shows the stair-stepping effect at angles of 15, 45, and 75 degrees. At zero degrees relative to the build plane, no stair steps are formed and surface roughness reaches its minimum value. Increasing the angle to 15 degrees creates long steps that produce a high surface roughness. As the angle is further increased, however, each step gets closer together and the roughness decreases. The steps disappear at an angle of 90 degrees relative to the build plane, but the roughness is still higher than at zero degrees. Variation between successive layers causes the greater roughness value.

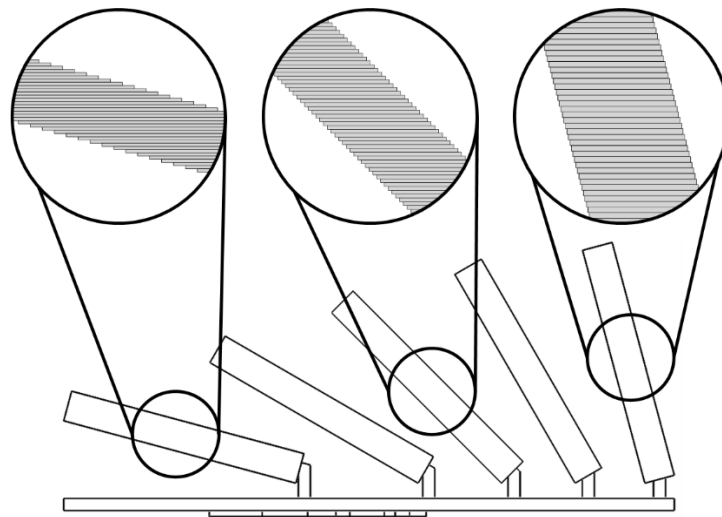


Figure 25: Observed stair-stepping at different angles relative to the build chamber

5.2.2 Linear Accuracy

Linear accuracy indicates how well the machine is able to hold linear dimensions with respect to the prescribed dimensions within the CAD model. Linear accuracy in each build

axis is determined by measuring the gap between successive walls, as depicted in Figure 26.

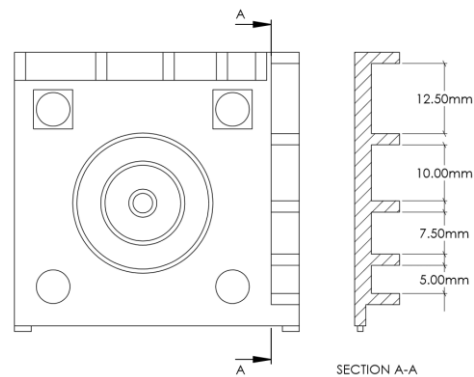


Figure 26: Linear accuracy test part

General Guidelines

- Linear accuracy is better along the Z-axis than the X and Y axes.
- The actual distance between features is generally less than the nominal values.
- Linear accuracy does not scale with size.

Accuracy

The linear accuracy of additively manufactured parts tends to understate dimensions by approximately 0.2mm. This trend appears to be independent of size and is consistent across the entire range of measurements. Features built on the interior of the build chamber are usually more undersized than those built along the perimeter. Accuracy along the Z-axis tends to be better than along the X and Y axes.

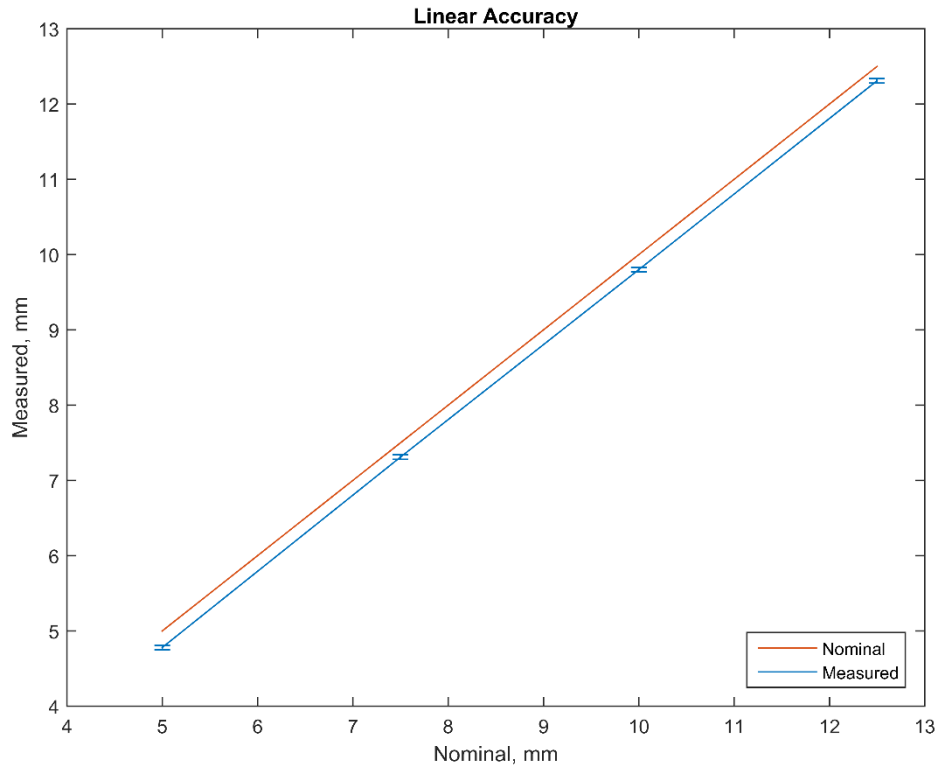


Figure 27: Linear accuracy trend for all test cubes

Significant Effects

Table 10 shows the significant factors generated from the ANOVA test for linear accuracy (see section 5.1.3 for an interpretation guide). Material and orientation are statistically significant for all values of linear accuracy tested.

Table 10: Significant effects for linear accuracy.

Linear Accuracy			
Distance (mm)			
5.0	7.5	10.0	12.5
M	M	M	M
O	O	O	O

Mean Differences

The full table for mean differences can be found in Appendix A. The results suggest that different materials can contribute up to 0.34mm of variation in linear accuracy. Similarly, orientation can influence the accuracy by as much as 0.10mm.

Explanation

Linear dimensions are undersized due to a phenomenon called oversintering. Oversintering occurs when the powder surrounding a part is unintentionally fused during the sintering process. The additional fused powder reduces the measured linear accuracy because accuracy is determined by the void space along the axis of interest (Figure 26). There are no observed scaling effects related to oversintering; at all measured distances the reported accuracy is approximately 0.20mm smaller than the nominal value. In addition to oversintering, laser spot size and layering effects can contribute to differences in accuracy for each of the three orientations. The laser spot size is typically 450 μ m in diameter while the thickness of each layer is 100 μ m. Linear dimensions along the Z-axis of the build chamber are more accurate because the dimension spreads across layers.

5.2.3 Gap Accuracy as a Function of Wall Thickness

Gap accuracy is determined by varying the gap size and the thickness of the wall through which the gap is created (Figure 28). The reported value corresponds to the gap measured along the axis of interest.

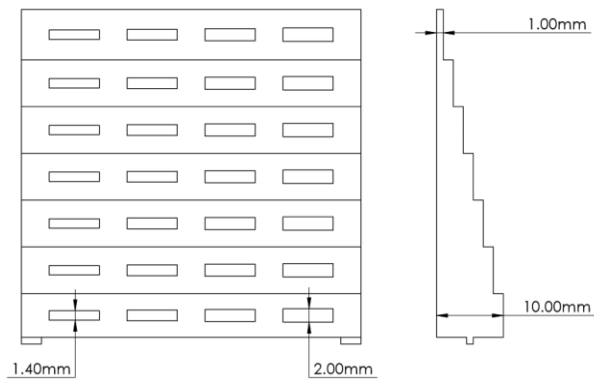


Figure 28: Gap accuracy as a function of wall thickness test part

General Guidelines

- Gaps are generally undersized compared to nominal values

Accuracy

Similar to linear accuracy, gaps tend to be undersized by approximately 0.20mm. There does not appear to be a significant dependence on wall thickness.

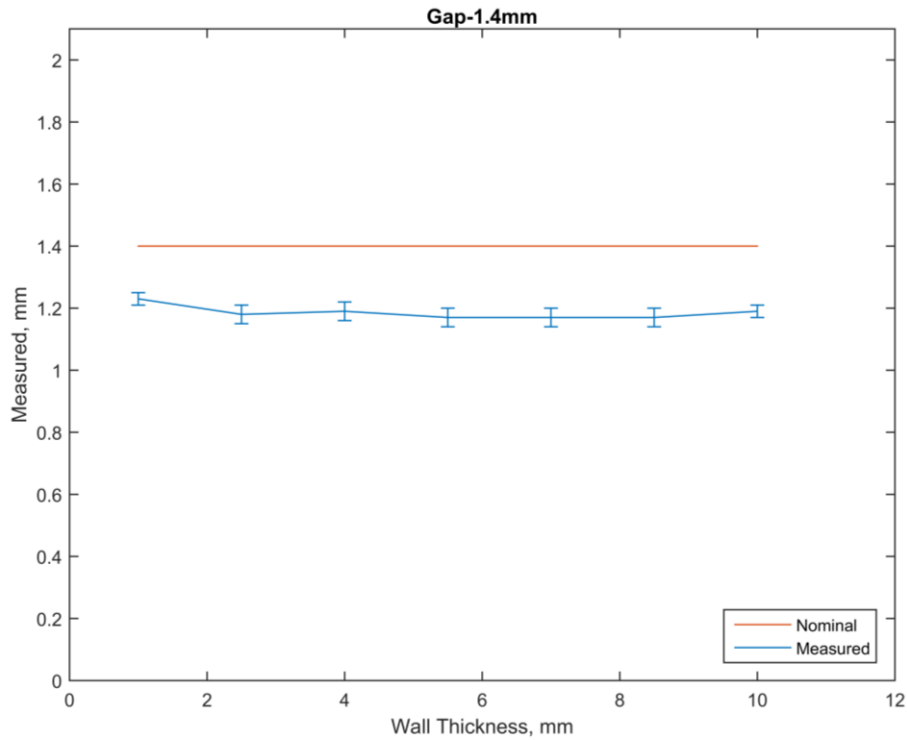


Figure 29: 1.4mm gap accuracy as a function of wall thickness for all test cubes

Significant Effects

The results of the ANOVA test for gap accuracy can be seen in Table 11 (see section 5.1.3 for an interpretation guide). Compared to linear accuracy, the significant effects for the accuracy of gaps are much more varied. Material choice is the only common significant factor between each of the gap distances and wall thicknesses.

Table 11: Significant effects for gap accuracy.

		Gap Accuracy						
		Wall Thickness (mm)						
		1.0	2.5	4.0	5.5	7.0	8.5	10.0
1.4mm Gap	M	M	M	M	M	M	M	M
	O	L	L	L	L	L	M*O	L
	L	O*L	M*O	M*O	M*O	M*O		
	M*O							
1.6mm Gap	M	M	M	M	M	M	M	M
	O	L	L	M*O	M*O	M*O	M*O	L
1.8mm Gap	M	M	M	M	M	M	M	M
	O	L	M*O	M*O				
		O*L						
2.0mm Gap	M	M	M	M	M	M	M	M
	O	L	L	L	L	L	M*O	L
	L		M*O	M*O	M*O	M*O		
			O*L					

Mean Differences

The full table for the mean differences associated with gap accuracy can be found in Appendix A. As shown in the significant effects, material selection is the most common source of variation. Changing materials can lead to mean differences as high as 0.36mm in some instances, but generally values are close to 0.20mm. FR PA 11 tends to undersize gaps the most, followed by GF PA 12 then PA 12.

Explanation

As with linear accuracy, oversintering appears to be the greatest contributing factor to the underreporting of gap accuracy. The results show that gaps tend to be smaller than the nominal dimension by approximately 0.2mm. Interestingly, there does not seem to be a

dependence on wall thickness. The under-sizing effect is relatively constant for all values of wall thickness and gap size for each material, but varies between materials. Oversintering appears to affect FR PA 11 more than PA 12 and GF PA 12. PA 11 has a higher melting point and smaller window of processing temperatures than PA 12 [23]. For this reason, FR PA 11 may be more susceptible to oversintering than either of the PA 12 blends.

5.2.4 Hole Diameter as a Function of Wall Thickness

Hole accuracy and resolution are determined by varying hole diameter as well as the thickness of the wall through which the hole is created (Figure 30). Hole resolution denotes the smallest hole that is reliably formed at each wall thickness. Accuracy provides quantitative comparisons of the mean hole diameter measured at each wall thickness for the two largest holes.

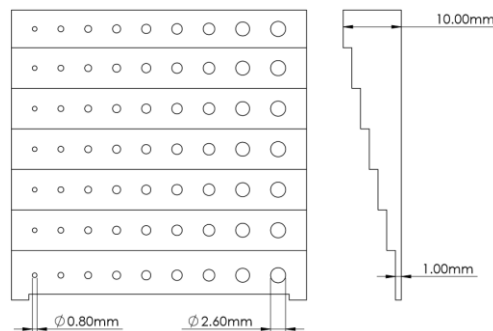


Figure 30: Hole diameter as a function of wall thickness test part

General Guidelines

- Holes are generally undersized compared to nominal values.
- Holes aligned along the Z-axis are the most undersized.
- Hole accuracy and resolution are dependent on wall thickness.
- Thinner walls resolve smaller holes, which are less undersized.

Accuracy

Accuracy is measured for hole diameters of 2.4mm and 2.6mm across all wall thicknesses. Hole diameters have a tendency to be undersized by approximately 0.4mm. The trend does appear to depend on the thickness of the wall, with thicker walls yielding smaller holes than thin.

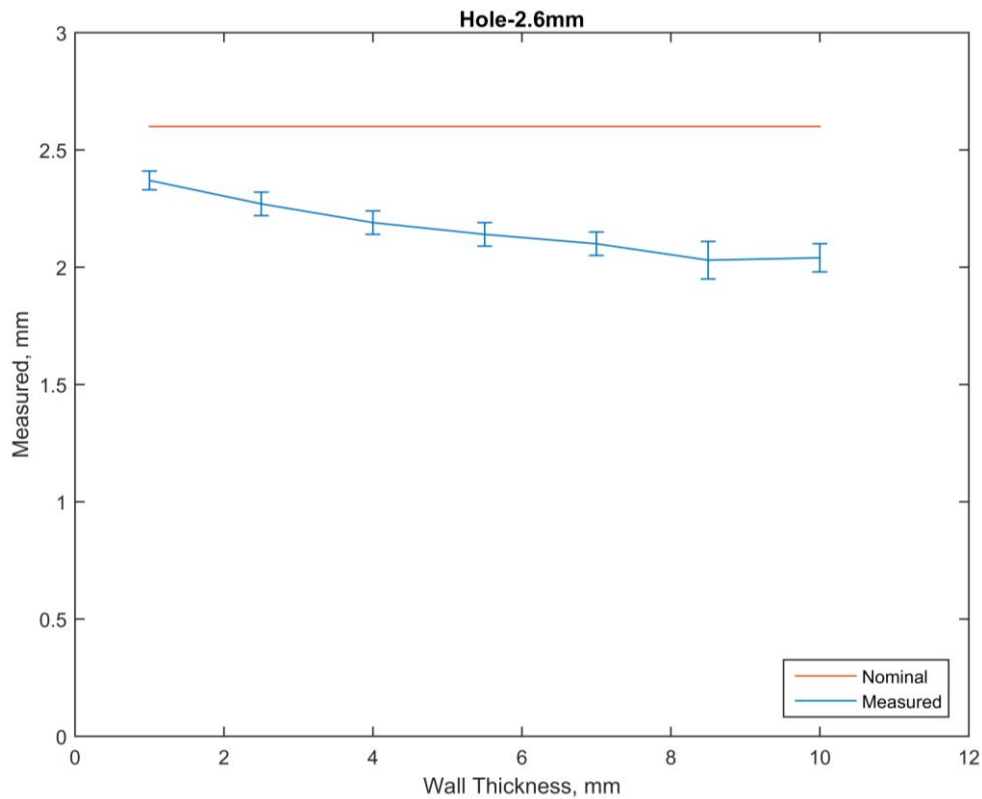


Figure 31: 2.6mm hole accuracy as a function of wall thickness for all test cubes

Resolution

Hole resolution appears to depend greatly on wall thickness. Thinner walls resolve smaller holes, and the smallest resolvable hole diameter tends to increase with wall thickness. In general, 1.0mm thick walls can reliably resolve (>75% of the time) 1.0mm holes. Conversely, 4.0mm thick walls can only resolve 1.8mm holes reliably.

Table 12: Hole diameter resolution as a function of wall thickness for all test cubes

		Holes						
		Hole Diameter (mm)						
		2.0	1.8	1.6	1.4	1.2	1.0	0.8
Wall Thickness (mm)	1.0	0.96	0.95	0.94	0.92	0.85	0.76	0.69
	2.5	0.91	0.88	0.86	0.78	0.7	0.57	0.41
	4.0	0.83	0.8	0.69	0.6	0.49	0.35	0.23
	5.5	0.68	0.6	0.55	0.43	0.35	0.24	0.05
	7.0	0.58	0.51	0.43	0.36	0.22	0.13	0.04
	8.5	0.5	0.43	0.37	0.26	0.16	0.07	0.04
	10.0	0.5	0.4	0.32	0.17	0.08	0.06	0.04

Significant Effects

Table 13 outlines the significant effects generated from the ANOVA test for hole accuracy (see section 5.1.3 for an interpretation guide). At every wall thickness for both the 2.4mm and 2.6mm holes, material and orientation are both statistically significant factors. The table also shows that location within the build chamber is significant for several of the holes measured. Additionally, some interaction effects can be seen at wall thicknesses 4.0mm and smaller.

Table 13: Significant effects for hole accuracy

		Hole Accuracy						
		Wall Thickness (mm)						
		1.0	2.5	4.0	5.5	7.0	8.5	10.0
2.6mm Hole	M	M	M	M	M	M	M	M
	O	O	O	O	O	O	O	O
	L	L	M*L	L				
	M*O							
	O*L							
2.4mm Hole	M	M	M	M	M	M	M	M
	O	O	O	O	O	O	O	O
	M*O		L					
	O*L							

Mean Differences

Appendix A shows the full table for mean differences associated with hole accuracy. Both material choice and hole orientation contributed to large observed differences in means. The mean differences were generally between 0.25mm and 0.35mm for both factors. PA 12 holes tend to be larger than both GF PA 12 and FR PA 11. Holes built in the Z-direction are the most undersized because the entire cross section of the hole lies in the plane of the laser path. The spot size of the laser is larger than the layer thickness, so holes are more undersized when they are built in-plane.

Explanation

Oversintering causes hole diameters to be smaller than the nominal value. However, in contrast to the gap accuracy results, hole diameters appear to have some dependence on wall thickness. The results indicate that holes through thick walls tend to be more undersized than the same diameter hole through thinner walls. This effect can be as large as 0.30mm between the 1.0mm and 10.0mm walls. One possible explanation for the additional reduction in measured diameter is that thick walls have more heat added during the sintering process than thin walls. With more residual heat, higher degrees of oversintering can be observed.

5.2.5 Thin Walls

Both accuracy and resolution are evaluated for thin walls. Two measurements are taken for thin walls – one at the base, and one at the middle –to test the accuracy of wall thickness when they are built in various orientations. Resolution is dictated by the thinnest wall that

can be reliably built. Thin walls are built with thicknesses ranging from 0.2mm to 0.8mm in increments of 0.1mm.

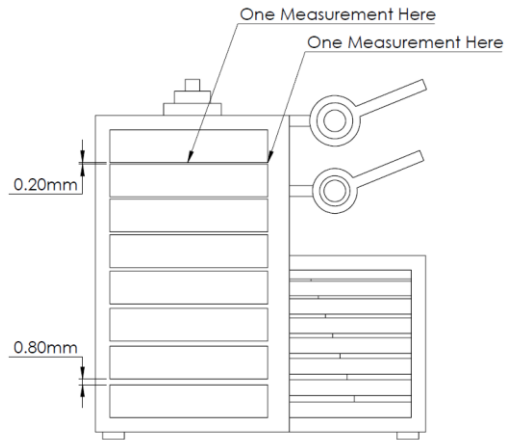


Figure 32: Thin wall test part

General Guidelines

- Thin walls are generally oversized compared to nominal.
- Walls at least 0.5 mm thick resolve well, while walls thinner than 0.5 mm generally do not resolve.
- Walls oriented parallel to the build plate (XY) are the most accurate.

Accuracy

Thin walls are usually oversized by approximately 0.2mm. This trend does not depend significantly on the thickness of the wall, but thicker walls are sometimes more oversized than thin walls.

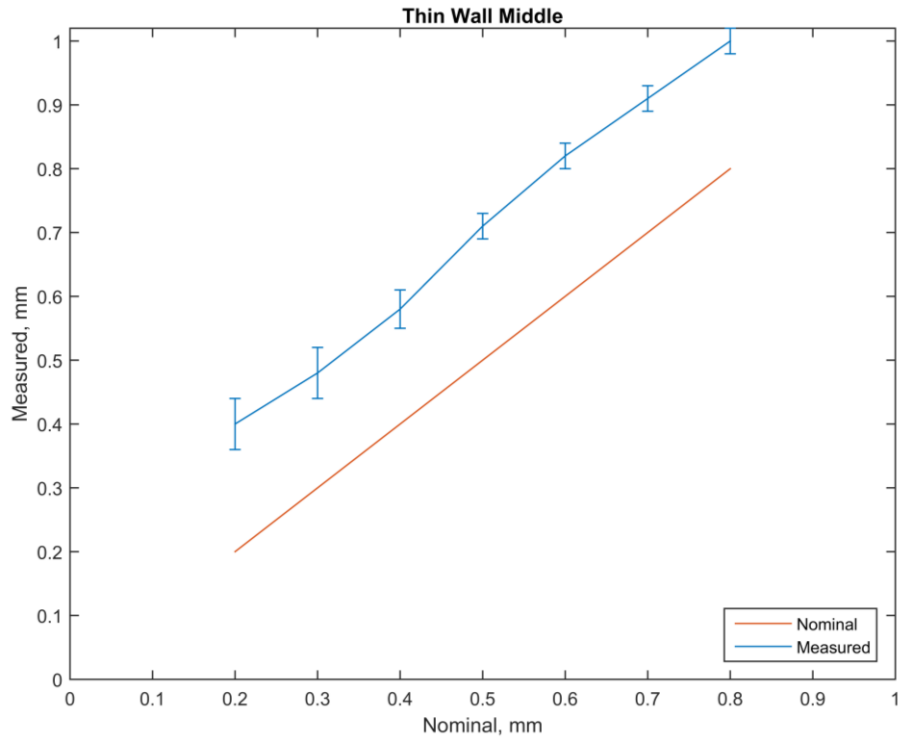


Figure 33: Thin wall accuracy for all test cubes. Measurements were taken in the middle of the wall.

Resolution

In general, the thinnest resolvable walls are 0.5mm thick. All walls thicker than 0.6mm resolved successfully.

Table 14: Thin wall resolution for all test cubes

Thin Walls	
Wall Thickness (mm)	Pass Proportion
0.2	0.34
0.3	0.39
0.4	0.49
0.5	0.92
0.6	1
0.7	1
0.8	1

Significant Effects

Table 15 lists the significant factors as determined by the ANOVA test (see section 5.1.3 for an interpretation guide). Measurements taken at one edge of the wall (outer) and at the center of the wall (middle) are shown. Interestingly, the two measurement locations do not have identical significant effects. However, material and orientation are significant factors for all of the walls measured.

Table 15: Significant effects for thin wall accuracy

Thin Wall Accuracy							
Wall Thickness (mm)							
	0.2	0.3	0.4	0.5	0.6	0.7	0.8
Thin Wall - Outer	M	M	M	M	M	M	M
	O	O	O	O	O	O	O
		L		L			
				M*O			
Thin Wall - Middle	M	M	M	M	M	M	M
	O	O	O	O	O	O	O
		L	M*O	M*O	M*L		

Mean Differences

The full table for mean differences is shown in Appendix A. PA 12 walls tend to be the most accurate dimensionally. Conversely, GF PA 12 walls can be up to 0.19mm thicker while FR PA 11 walls are as much as 0.26mm thicker. For orientation, XY walls are the most accurate. XZ and YZ walls are generally 0.10 to 0.12mm thicker by comparison.

Explanation

As with the other features, oversintering plays a large role in the accuracy of thin walls. In this case, however, oversintering causes the walls to be larger than their nominal dimension. This is because walls are an “additive” feature where the laser scans the feature geometry. Gaps and holes are “subtractive” features where the feature geometry is

determined by voids in the laser scan area. Oversintering leads to “subtractive” features being undersized and “additive” features being oversized.

The resolution results for thin walls show a strong dependence on orientation. Tables 16-18 depict the observed resolution when filtered for each of the three orientations. Walls built in the XY orientation can be resolved at thicknesses as small as 0.2mm, while walls built in either the XZ or YZ orientations can only reliably resolve at thicknesses 0.5mm and greater. Walls oriented in the XY plane of the build chamber achieve better resolution because they lie in the same plane as the layers in SLS. The thickness of the layers, then, drives the resolution. For polymer PBF, layers are typically 0.1mm thick. Therefore, a 0.2mm wall in the XY plane is made up of two layers. XZ and YZ oriented walls are both out of plane with respect to the layers. During the build process, the laser traces out the thickness at each layer. For these orientations, the spot size of the laser determines the minimum resolution of thin walls. SLS lasers typically have a spot size of 0.45mm in diameter, which is consistent with the XZ and YZ resolution results shown in Tables 17 and 18.

Table 16: Resolution of thin walls built in the XY orientation

XY Thin Walls	
Wall Thickness (mm)	Pass Proportion
0.2	0.77
0.3	0.9
0.4	0.98
0.5	1
0.6	1
0.7	1
0.8	1

Table 17: Resolution of thin walls built in the XZ orientation

XZ Thin Walls	
Wall Thickness (mm)	Pass Proportion
0.2	0.13
0.3	0.13
0.4	0.23
0.5	0.85
0.6	1
0.7	1
0.8	1

Table 18: Resolution of thin walls built in the YZ orientation

YZ Thin Walls	
Wall Thickness (mm)	Pass Proportion
0.2	0.13
0.3	0.15
0.4	0.25
0.5	0.9
0.6	1
0.7	1
0.8	1

5.2.6 Thin Rods

Three types of rods are tested for resolution. Supported rods are connected to side walls at both ends, while unsupported rods are cantilevered. Aspect ratios (length/diameter) of 5 and 10 are used for short and long unsupported rods, respectively, with rod diameters varying from 0.3mm to 0.9mm in 0.1mm increments.

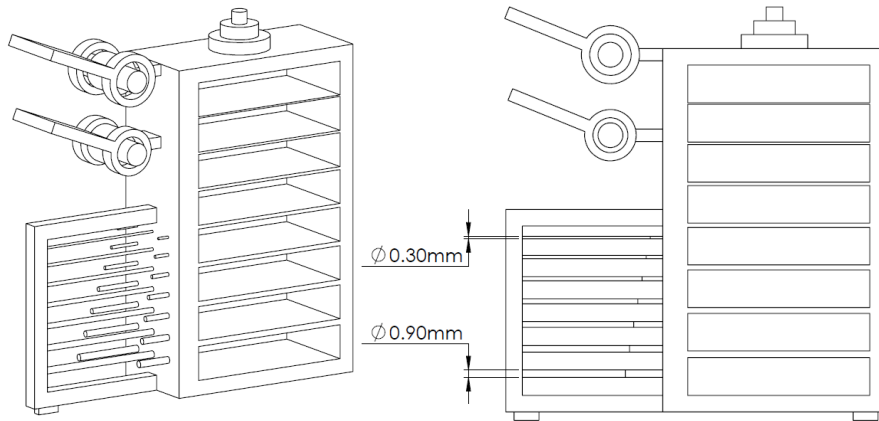


Figure 34: Thin rod test part

General Guidelines

- Neither support type nor aspect ratio significantly affect the resolution of rods.
- Rods at least 0.6 mm in diameter resolve well, while rods thinner than 0.6 mm generally do not resolve.

Resolution

No significant relationship is observed between the support conditions and the ability to resolve thin rods. In order to ensure reliable resolution of thin rods, they should generally be at least 0.6mm in diameter. Smaller rods tend to fail or leave an “empty” spot in their place.

Table 19: Resolution of supported rods for all test cubes

Supported Rods	
Rod Diameter (mm)	Pass Proportion
0.3	0.42
0.4	0.34
0.5	0.68
0.6	0.96
0.7	0.99
0.8	0.99
0.9	0.99

Table 20: Resolution of unsupported rods with an aspect ratio of 10 for all test cubes

Unsupported Rods - Long	
Rod Diameter (mm)	Pass Proportion
0.3	0.42
0.4	0.35
0.5	0.69
0.6	0.97
0.7	0.99
0.8	0.99
0.9	0.99

Table 21: Resolution of unsupported rods with an aspect ratio of 5 for all test cubes

Unsupported Rods - Short	
Rod Diameter (mm)	Pass Proportion
0.3	0.42
0.4	0.35
0.5	0.68
0.6	0.97
0.7	0.99
0.8	0.99
0.9	0.99

Explanation

The resolution results for thin rods suggest that neither aspect ratio nor being supported at both ends has a substantial effect on resolution. The self-supporting SLS powder bed secures the rods in place during the build process, eliminating the effect of unsupported length. Rods can generally be resolved reliably at diameters greater than 0.5mm. Similar to thin walls built in the XZ and YZ orientations, the spot size dominates thin rod resolution.

5.2.7 Hinges

Two hinge designs are tested by varying the gap between the shaft of the hinge and the knuckle. The dimensions are shown in Figure 35. The hinges are tested by checking whether they can move freely.

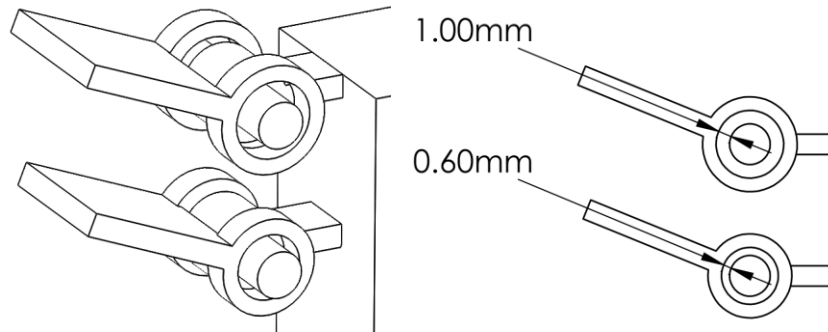


Figure 35: Hinge test part

General Guidelines

- Shaft clearances of 0.6mm generally do not resolve, while 1.0mm clearances do resolve.

Resolution

The results of the study concluded that a 1.0mm shaft clearance is generally sufficient for creating mechanical hinges. Conversely, it is not recommended to design hinges with only a 0.6mm clearance because the knuckle will most likely fuse to the shaft, rendering it immobile.

Table 22: Hinge resolution at shaft clearances of 0.6 and 1.0mm for all test cubes

Hinges	
Shaft Clearance (mm)	
1.0	0.6
0.85	0.22

Explanation

Hinges with a shaft clearance of 1.0mm generally resolve successfully while those with a shaft clearance of 0.6mm generally do not. As seen in the linear accuracy and gap accuracy results, oversintering tends to affect measurement results by about 0.2mm. Using this rule, all hinges with a shaft clearance greater than 0.6mm should be able to move freely. However, the results suggest that a shaft clearance closer to 1.0mm is necessary. The design of the hinge accounts for this discrepancy. For a hinge to move freely, there needs to be a small amount of unfused powder between the shaft and the knuckle. Consequently, this small gap, referred to here as the shaft clearance, also allows additional heat to be trapped. The resulting effect is that more oversintering occurs than would otherwise be expected. For this reason, the spacing of features relative to each other on an SLS part is important to ensure they do not become fused together.

5.2.8 Lettering

Many designers wish to include lettering on the surfaces of parts. Both embossed and raised lettering is tested at letter depths of 0.5mm to 2.5mm and font sizes ranging from 10pt to 18pt. The font is Arial (Regular), a sans-serif font. Both uppercase and lowercase forms of the letter “A” are used as the test font, as shown in Figure 36.

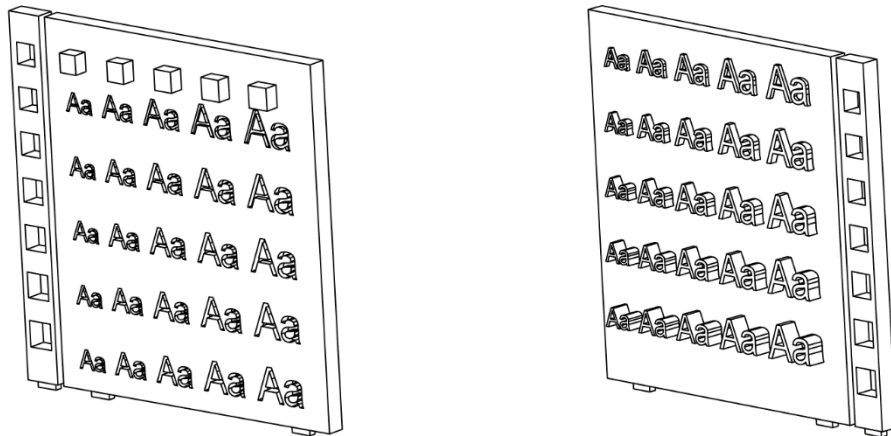


Figure 36: Raised and embossed lettering test part

General Guidelines

- Embossed lettering yields superior resolution to raised lettering.
- Lettering resolution improves as font size increases.

Resolution

Lettering resolution does not appear to depend significantly on the depth of the emboss/extrude, but depends substantially on the size of the font. Embossed lettering reliably resolves nearly all font sizes at all emboss depths. For this reason, a designer should consider embossed lettering as opposed to raised when adding text to a part that is additively manufactured using selective laser sintering. If raised lettering is desired, fonts larger than 16pt should be used.

Table 23: Resolution of embossed lettering for all test cubes

		Embossed Lettering				
		Font Size (pt)				
		10	12	14	16	18
Emboss Depth (mm)	0.5					
	1.0					
	1.5					
	2.0					
	2.5					

Table 24: Resolution of raised lettering for all test cubes

		Raised Lettering				
		Font Size (pt)				
		10	12	14	16	18
Extruded Depth (mm)	0.5					
	1.0					
	1.5					
	2.0					
	2.5					

Explanation

Embossed lettering is preferred to raised lettering because raised lettering requires many fine “positive” features. At font sizes below 16pt the features are too small to be resolved by the laser spot and result in significant defects. Embossed lettering is less susceptible to these defects because only the feature “negative” is scanned by the laser. Raised letters are in many ways similar to unsupported thin rods. As shown in the thin rod results, unsupported length does not generally affect resolution. It is not surprising then, that the resolution of raised letters does not depend on the height at which they are extruded.

5.2.9 Snap Fits

The offset required for mechanical snap fits is determined by testing an extruded square peg against slots of varying size. Square pegs of 3.0mm nominal width are tested against slots of 2.9mm to 3.5mm nominal width in increments of 0.1mm.

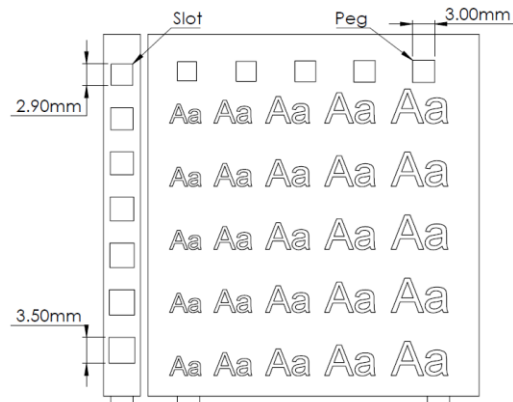


Figure 37: Mechanical snap fit test part

General Guidelines

- Offsets between peg and slot between 0.15 mm and 0.2 mm perform best

Resolution

In general, when incorporating mechanical snap fits into a design, an offset of 0.15mm to 0.2mm should be used between the peg and slot. An example design is shown in Figure 38.

Table 25: Snap fit resolution for all test cubes. Green boxes indicate the offsets that correspond to the best fit between the peg and slots.

Snap Fits						
Offset (mm)						
-0.05	0	0.05	0.1	0.15	0.2	0.25
0.09	0.07	0.1	0.13	0.26	0.23	0.12

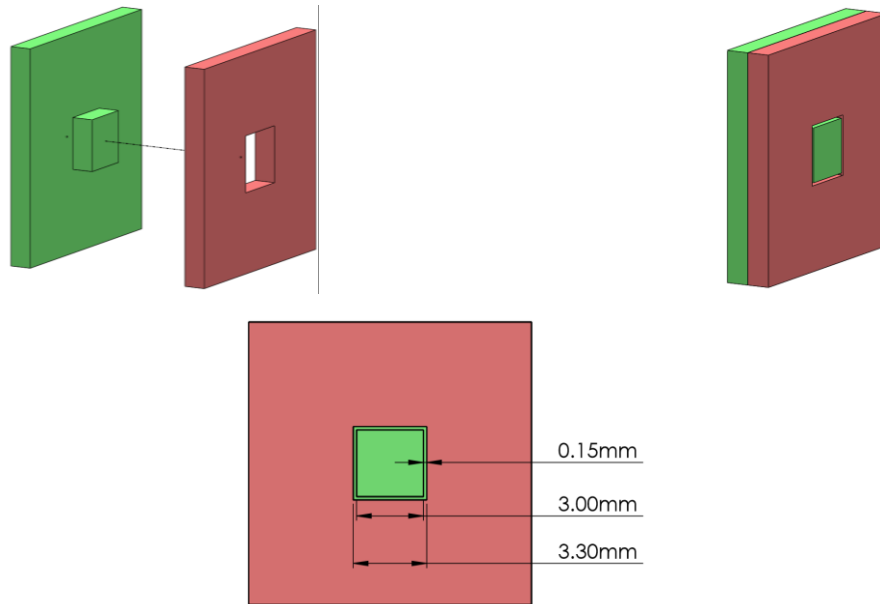


Figure 38: Convention used for analyzing snap fits

Explanation

The theoretical ideal snap fit offset is slightly less than 0mm. A slightly negative offset theoretically allows a snug fit between the peg and slot. However, the results indicate that a snap fit designed for SLS requires an offset between 0.15 and 0.2mm. Oversintering causes both the peg to be oversized and the slot to be undersized. The linear accuracy and gap accuracy results suggest an oversintering effect of 0.2mm. This is consistent with the snap fit results which show an ideal offset slightly less than 0.2mm. Oversintering, in effect, has shifted the theoretical ideal offset by 0.2mm.

5.3 Machine Variability

As outlined in Section 3.5, five test cube replicates are built on one machine, and three replicates are built on a second machine in an effort to assess variability between machines. However, due to manufacturing constraints, the machines used for “Machine 1” and

“Machine 2” vary for each material. Therefore, machine variability must be assessed on a per-material basis.

Machine variability is evaluated by implementing an analysis of variance test with multiple comparisons, just as with the other input factors. Table 26-Table 28 show the machine variability for gap accuracy, hole accuracy, and thin wall accuracy. Machine variability is not statistically significant for linear accuracy. In each of the tables, “Machine Significant” implies machine-to-machine variation is statistically significant for a particular feature size. Immediately to the right of the text, the mean difference between the machines is given.

Table 26: Gap accuracy machine variability analysis

		Gap Accuracy			
		Gap Distance (mm)			
		1.4	1.6	1.8	2.0
		PA 12			
Wall Thickness (mm)	1.0		Machine Significant 0.07		
	2.5				
	4.0				
	5.5				
	7.0	Machine Significant 0.05			Machine Significant 0.06
	8.5	Machine Significant 0.08	Machine Significant 0.08	Machine Significant 0.09	Machine Significant 0.06
	10.0	Machine Significant 0.07	Machine Significant 0.06		Machine Significant 0.07
		GF PA 12			
Wall Thickness (mm)	1.0				
	2.5	Machine Significant 0.08	Machine Significant 0.08	Machine Significant 0.11	Machine Significant 0.08
	4.0	Machine Significant 0.08	Machine Significant 0.09	Machine Significant 0.1	Machine Significant 0.1
	5.5	Machine Significant 0.06	Machine Significant 0.09	Machine Significant 0.11	Machine Significant 0.1
	7.0	Machine Significant 0.06	Machine Significant 0.08	Machine Significant 0.09	Machine Significant 0.07
	8.5	Machine Significant 0.07	Machine Significant 0.11	Machine Significant 0.1	Machine Significant 0.1
		10.0	Machine Significant 0.07	Machine Significant 0.09	Machine Significant 0.09
		FR PA 11			
Wall Thickness (mm)	1.0	Machine Significant 0.15	Machine Significant 0.16	Machine Significant 0.15	Machine Significant 0.17
	2.5	Machine Significant 0.06			
	4.0				
	5.5				
	7.0				
	8.5				
		10.0	Machine Significant 0.09	Machine Significant 0.09	Machine Significant 0.09

Table 27: Hole accuracy machine variability analysis

		Hole Accuracy	
		Hole Diameter (mm)	
		2.6	2.4
		PA 12	
Wall Thickness (mm)	1.0		
	2.5		
	4.0		
	5.5		
	7.0		
	8.5		
	10.0		
		GF PA 12	
Wall Thickness (mm)	1.0	Machine Significant	0.13
	2.5		
	4.0		
	5.5		
	7.0		
	8.5		
	10.0		
		FR PA 11	
Wall Thickness (mm)	1.0	Machine Significant	0.12
	2.5		
	4.0		
	5.5		
	7.0		
	8.5		
	10.0		Machine Significant

Table 28: Thin wall accuracy machine variability analysis

		Wall Thickness			
		Outer		Middle	
		PA 12			
Wall Thickness (mm)	0.2				
	0.3				
	0.4				
	0.5	Machine Significant	0.11	Machine Significant	0.12
	0.6				
	0.7	Machine Significant	0.11	Machine Significant	0.14
	0.8	Machine Significant	0.11	Machine Significant	0.14
		GF PA 12			
Wall Thickness (mm)	0.2				
	0.3				
	0.4				
	0.5	Machine Significant	0.09	Machine Significant	0.07
	0.6			Machine Significant	0.04
	0.7				
	0.8				
		FR PA 11			
Wall Thickness (mm)	0.2				
	0.3				
	0.4				
	0.5				
	0.6				
	0.7				
	0.8				

The results suggest that machine variation is not consistent across features and materials. For example, machine variation for GF PA 12 is statistically significant for nearly all gap sizes, but only one hole. This can have implications to a designer creating a part for polymer SLS. Depending on the part design, changing machines may have a stronger effect on certain features over others. The results also show that machine variability typically influences accuracy by between 0.08 and 0.11mm but can be as high as 0.2mm. Although the results suggest machine variability can be inconsistent, in many cases statistically significant differences in feature accuracy are seen. The effects of switching machines therefore cannot be ignored.

Chapter 6 Public Accessibility of Design Guidelines

6.1 Introduction

One of the barriers to widespread adoption of polymer PBF is that there is no comprehensive repository containing information on the process. A publicly accessible compilation of process descriptions and design guidelines is needed for designers both in the process selection stage and part realization stage of the design cycle. For designers who are unfamiliar with additive manufacturing, matching part design and manufacturing process can be challenging. Currently, DFAM information is either scattered across multiple sources, or proprietary to specific institutions.

This research seeks to establish a web-based platform that can be accessed by any designer in an effort to ease the DFAM process for polymer PBF. The design guidelines presented in Chapter 5 form the basis for the web tool. As an online application, the PBF web tool is freely available to the public. This tool provides unprecedented access to comprehensive, statistically robust polymer PBF design guidelines. The web tool can be accessed at <http://DesignForAM.me.utexas.edu>.

6.2 Web Tool

Figure 39 shows the present layout of the DFAM web tool. The tool focuses primarily on polymer PBF, but it can be extended to other processes as well. DFAM studies for fused deposition modeling (FDM) and metal PBF are being added. From the home page, the user can navigate to different pages based on the intended application. For polymer PBF, the user can be directed to a page containing a version of the design guidelines outlined in Chapter 5 of this thesis that has been modified to fit the web platform. Just as the design

guidelines are ordered from general to specific, the web tool first presents the user with high level guidelines for each feature. The “Process Overview” section provides general information about polymer PBF and is intended for designers who are unfamiliar with the process. A page is also dedicated to the measurement methods used to populate the design guidelines, similar to Chapter 4 of this thesis. For designers who wish to print physical copies of the material, there are links to “printer-friendly” versions of both the design guidelines and measurement methods.

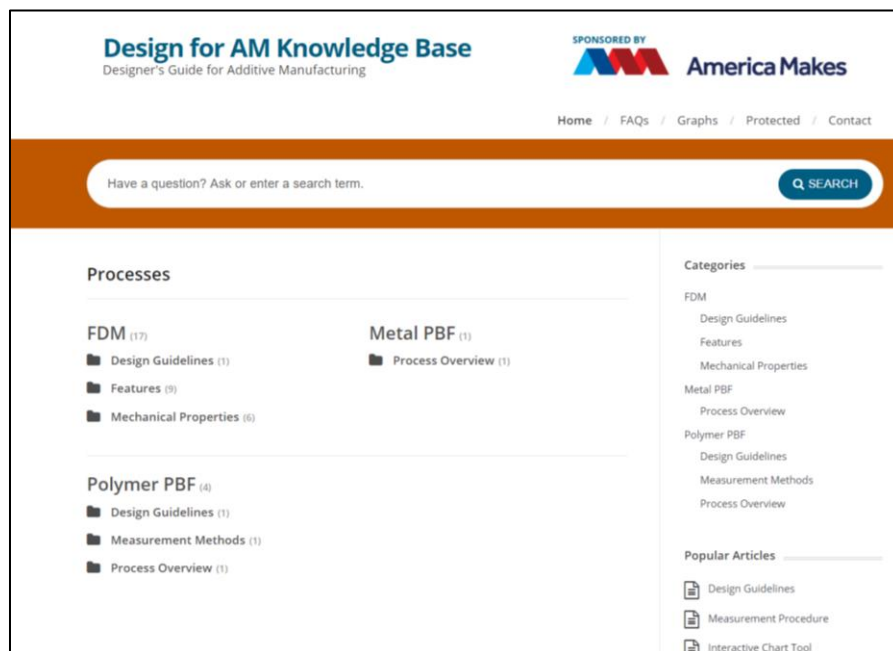


Figure 39: Web tool layout

The web tool is implemented using the WordPress platform, enabling it to be continually updated as new DFAM information is generated. Although public accessibility is one of the main tenets of the web tool, protecting the integrity of the results is highly important. Therefore, editing privileges for the website are password protected. This ensures only trusted individuals can access and modify the information.

6.3 Interactive Capability

In some cases, designers may want to observe the effects of different process parameters on certain features. The web tool includes an interactive component that enables the designer to display trends based on selected input parameters. An example of the interactive chart tool is shown in Figure 40. In this case, the designer has selected GF PA 12 as the material, “XY” as the orientation, and is not controlling for location within the build chamber. By selecting different options from the dropdown menu, the designer can compare the relative effects of any input parameter combination. For instance, if a particular design relies on the ability to resolve thin walls in different orientations, the designer can quickly assess thinnest observable walls in each orientation. Figure 41 shows the updated graph selection when the orientation is changed from “XY” to “XZ.” It can be seen that GF PA 12 walls built along the “XY” axes of the build chamber (Figure 40) successfully resolved for all thicknesses measured in the study. Conversely, when the orientation is changed to “XZ” (Figure 41), only walls greater than 0.5mm resolved successfully. This same method of comparison can be used to observe the effects of any combination of input parameters that were included in the metrology study.

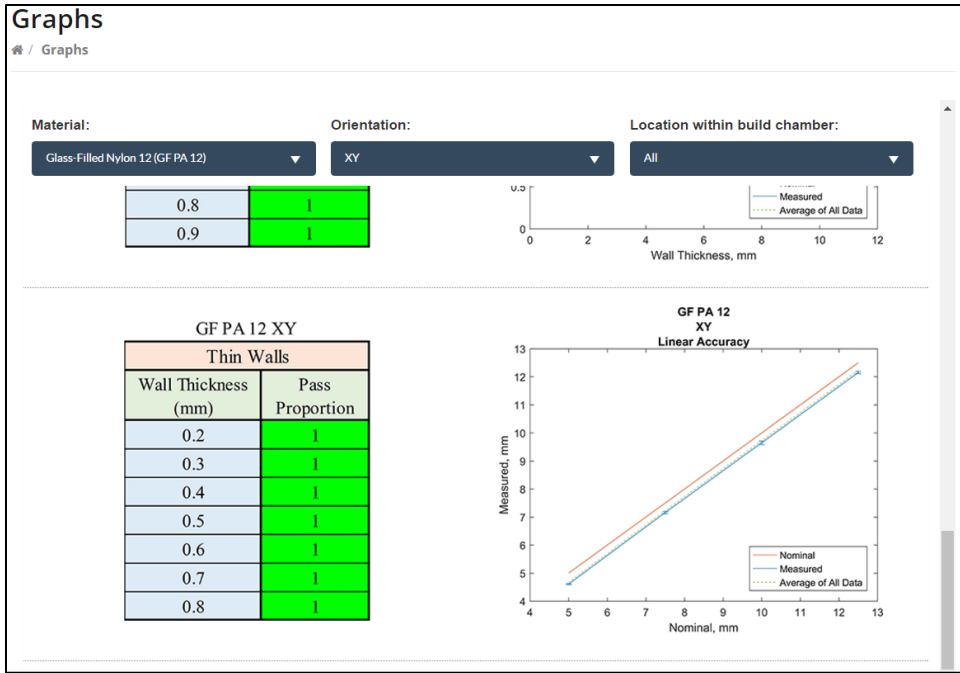


Figure 40: Interactive web tool filtered to display the results for all cubes built in GF PA 12 and in the XY orientation



Figure 41: Interactive chart tool filtered to display results for all cubes built in GF PA 12 and in the XZ orientation

The level of detail offered by this tool can only be achieved in the form of an interactive capability, as each combination of inputs has a unique set of associated graphs and charts. In fact, in order to account for all input combinations in the polymer study, more than 800 graphs and charts are needed. It is difficult for a designer to make sense of such a large number of figures, but the interactive tool allows for quick comparisons of parameters of interest. The interactive component of the web tool puts the power in the hands of the designer, showing how each processing parameter or combination of parameters can affect part quality.

Chapter 7 Closure

7.1 Summary

This research sought to investigate the impacts of various processing parameters on the part quality in polymer selective laser sintering. Previous efforts to characterize the SLS process were insufficient either in the statistical reliability of the results or in the features considered. This work was aimed at expanding previous metrology studies to develop a more complete understanding of SLS.

Chapter 1 established the need for a statistical characterization of the SLS process to aid designers in creating parts for AM. A comparison of several previous test parts revealed an opportunity for an improved metrology study for polymer PBF. Standard test parts, such as the part proposed by Moylan et al., did not fully utilize or investigate certain process-specific capabilities [6]. The SLS test parts developed by Govett et al. were too large to generate enough replicates for a statistical characterization [8]. These previous efforts exposed a need for an SLS test part that was both comprehensive and compact.

The design of the polymer PBF test part was discussed in Chapter 2. The test part consisted of five panels of features attached to a common base. After being built, the panels were removed and measured separately. The features incorporated into the test cube design were chosen because they are common in typical engineering designs. The feature sizes were determined based on the results of previous metrology studies. The sizes were intended to capture both resolution and accuracy information in order to make the most efficient use of the test cube. The resulting feature density (number of features per unit

volume) of the proposed test cube was nearly five times higher than that of any of the previous test parts investigated.

Chapter 3 outlined the metrology study that was implemented to characterize the SLS process. The test part was used in a factorial-style experiment consisting of three different materials, three different build orientations, and two locations within the build chamber. Five replicates of the test part were built on a single machine, and three on a different machine. In total, 144 test parts were built using 3D Systems Sinterstation machines.

Chapter 4 detailed the various measurement techniques used in the metrology study. It was important to pair the appropriate measurement method with each feature to ensure meaningful results. Resolution was determined through visual inspection of the features and assigned a “Pass” or “Fail” rating. Measurement techniques for the accuracy results varied in complexity. Most of the accuracy data was taken using iGaging digital calipers. Complicated measurements such as surface roughness, however, required more advanced measurement methods. Surface roughness was measured using an optical surface profilometer. Lastly, a Gage R&R study was conducted to assess the variability in the caliper measurements. The results of the Gage R&R showed that the measurements for linear accuracy and wall thickness both fell within the acceptable range of variation. Gap accuracy, however, was slightly outside the generally accepted range. Therefore the results for gap accuracy contained additional variation attributed to the measurement system that may not have been associated with the actual part to part variation.

The design guidelines for each feature type were presented in Chapter 5. The structure of the guidelines began by providing general design guidelines and increasing in detail.

This format added flexibility to the guidelines so that designers could use them differently based on the intended application. The results of the metrology study showed that material choice and orientation of the feature in the build chamber were generally the most influential factors. Location within the build chamber was not a statistically significant effect for most features. Lastly, machine variation was assessed on a per-material basis. The results suggested that machine variation could be statistically significant, but the effects were not consistent across feature types.

Chapter 6 described the DFAM web tool. Compiling each of the measurement results and design guidelines, the web tool allowed the polymer PBF metrology results to be publicly accessible. The web tool incorporated an interactive feature that could be used by designers to investigate the effects of specific combinations of process parameters on part quality. The web tool created a platform to host DFAM knowledge that did not previously exist. The tool was designed on a common platform that could be continually updated with new DFAM resources.

7.2 Implications

Additive manufacturing offers many opportunities for the design of complex parts that are unachievable through any other manufacturing process. However, there are no comprehensive studies available in the public domain that thoroughly investigate the capabilities and limitations of each AM process. This leaves designers with a limited understanding of AM, which could result in unnecessary design iterations. Process-specific design guidelines are needed to address these lapses in AM knowledge and make DFAM easier.

Each AM technology has its own unique capabilities and challenges specific to the process. Consequently, a “one-size-fits-all” universal test part is unable to effectively describe each process. The polymer test part proposed here is specific to SLS and would not be well-suited for other technologies. Even metal PBF would be unable to build it due to the need for support material. Therefore, test parts are most effective when they are designed specifically for the process they seek to characterize. Customized test parts for each AM process can provide designers with the information needed not only to select the appropriate process for each design but also to utilize the process to its fullest extent.

Comprehensive metrology studies are necessary when characterizing an AM process. The polymer study presented in this thesis is one example of how DFAM guidelines benefit from rigorous characterization efforts. Building many test part replicates provides statistical information that can be integrated into design guidelines. Generating statistically significant results requires large amounts of measurements to be collected and analyzed. Making sense of such a high volume of data highlights the need to present the design guidelines in a manner that can be easily understood by a designer. Color-coded charts for resolution information and trend graphs for feature accuracy are one visualization method for designers to quickly understand the tradeoffs associated with each design feature. The results of the polymer PBF metrology study as well as others within this America Makes initiative are best suited to a web-based platform to allow public access to DFAM guidelines. Updating this web tool over time can establish a single platform for DFAM guidelines specific to all AM processes.

7.3 Future Work

Further investigation of the complex features from the polymer test cube is needed to complete the SLS characterization study. Namely, the dome, cone, and cylindricity features must be measured using a coordinate measuring machine, or 3D optical scanner. Moreover, the metrology study could be broadened by building additional copies of the test part. In the extended study, different machines, machine manufacturers, and other processing parameters could be implemented to develop a more complete assessment of the statistical results.

This test part is aimed at gathering information that is useful to designers. The features incorporated were selected to meet the needs for designers creating parts for polymer PBF. However, other test parts can be designed to assist process engineers in tuning machine parameters. A test part combined with a statistical database can be used to compare the part quality associated with a particular machine against other commercial machines. Process engineers can use this information as a check to determine whether certain machines are performing adequately or if maintenance is required.

Opportunities also exist to incorporate additional features not included in the present form of the test cube. Future studies could add functional features such as compliant structures, gears, and springs. Another opportunity for polymer PBF test parts would be to investigate various lattice structure designs. Strength and stiffness information could be gathered through mechanical testing, and geometric variation could be linked to performance variation.

Process-specific test parts analogous to the test cube used for polymer PBF are needed to characterize other AM processes. By performing similar statistically robust metrology studies, a database of DFAM knowledge can be created. Such efforts are currently in place to add FDM and metal PBF results to the online web tool. The web tool provides a platform to combine all existing AM knowledge from every process. This has the potential to be an extremely valuable tool for designers, as no comprehensive database exists. Compiling DFAM guidelines into a single interface allows designers to compare and contrast the various processes without the need to search multiple databases.

Appendix A

Tables 29-32 show the mean differences discussed in Sections 5.2.2-5.2.5. Refer to section 5.1.4 for an interpretation of mean differences.

Table 29: Linear Accuracy mean differences

Linear Accuracy							
Distance (mm)							
5.0		7.5		10.0		12.5	
PA 12-GF PA 12	0.24	PA 12-GF PA 12	0.24	PA 12-GF PA 12	0.26	PA 12-GF PA 12	0.26
PA 12-FR PA 11	0.34	PA 12-FR PA 11	0.34	PA 12-FR PA 11	0.34	PA 12-FR PA 11	0.34
GF PA 12-FR PA 11	0.1	GF PA 12-FR PA 11	0.1	GF PA 12-FR PA 11	0.08	GF PA 12-FR PA 11	0.07
XY-XZ	-0.08	XY-XZ	-0.1	XY-YZ	-0.06	XY-XZ	-0.1
XY-YZ	-0.07	XY-YZ	-0.1			XY-YZ	-0.1

Table 30: Gap accuracy mean differences

Gap Accuracy								
Wall Thickness (mm)	1.4mm Gap		1.6mm Gap		1.8mm Gap		2.0mm Gap	
1.0	PA 12-GF PA 12	0.16	PA 12-GF PA 12	0.15	PA 12-GF PA 12	0.17	PA 12-GF PA 12	0.18
	PA 12-FR PA 11	0.16	PA 12-FR PA 11	0.18	PA 12-FR PA 11	0.19	PA 12-FR PA 11	0.22
	XY-YZ	-0.07	XY-YZ	-0.11	XY-YZ	-0.11	XY-YZ	-0.11
	XZ-YZ	-0.07					XZ-YZ	-0.08
	I-E					I-E	0.04	
2.5	PA 12-GF PA 12	0.21	PA 12-GF PA 12	0.19	PA 12-GF PA 12	0.19	PA 12-GF PA 12	0.21
	PA 12-FR PA 11	0.33	PA 12-FR PA 11	0.31	PA 12-FR PA 11	0.31	PA 12-FR PA 11	0.32
	GF PA 12-FR PA	0.12	GF PA 12-FR PA 11	0.11	GF PA 12-FR PA 11	0.12	GF PA 12-FR PA 11	0.11
	I-E	0.05					I-E	0.06
4.0	PA 12-GF PA 12	0.21	PA 12-GF PA 12	0.21	PA 12-GF PA 12	0.19	PA 12-GF PA 12	0.23
	PA 12-FR PA 11	0.31	PA 12-FR PA 11	0.32	PA 12-FR PA 11	0.33	PA 12-FR PA 11	0.37
	GF PA 12-FR PA	0.1	GF PA 12-FR PA 11	0.11	GF PA 12-FR PA 11	0.14	GF PA 12-FR PA 11	0.14
	I-E	0.04					I-E	0.04
5.5	PA 12-GF PA 12	0.19	PA 12-GF PA 12	0.2	PA 12-GF PA 12	0.19	PA 12-GF PA 12	0.22
	PA 12-FR PA 11	0.32	PA 12-FR PA 11	0.32	PA 12-FR PA 11	0.32	PA 12-FR PA 11	0.35
	GF PA 12-FR PA	0.13	GF PA 12-FR PA 11	0.12	GF PA 12-FR PA 11	0.13	GF PA 12-FR PA 11	0.13
	I-E	0.03					I-E	0.03
7.0	PA 12-GF PA 12	0.17	PA 12-GF PA 12	0.19	PA 12-GF PA 12	0.19	PA 12-GF PA 12	0.2
	PA 12-FR PA 11	0.32	PA 12-FR PA 11	0.3	PA 12-FR PA 11	0.33	PA 12-FR PA 11	0.36
	GF PA 12-FR PA	0.15	GF PA 12-FR PA 11	0.11	GF PA 12-FR PA 11	0.13	GF PA 12-FR PA 11	0.16
	I-E	0.04					I-E	0.04
8.5	PA 12-GF PA 12	0.16	PA 12-GF PA 12	0.17	PA 12-GF PA 12	0.16	PA 12-GF PA 12	0.19
	PA 12-FR PA 11	0.29	PA 12-FR PA 11	0.29	PA 12-FR PA 11	0.3	PA 12-FR PA 11	0.34
	GF PA 12-FR PA	0.13	GF PA 12-FR PA 11	0.12	GF PA 12-FR PA 11	0.14	GF PA 12-FR PA 11	0.16
10.0	PA 12-GF PA 12	0.15	PA 12-GF PA 12	0.16	PA 12-GF PA 12	0.13	PA 12-GF PA 12	0.16
	PA 12-FR PA 11	0.26	PA 12-FR PA 11	0.25	PA 12-FR PA 11	0.26	PA 12-FR PA 11	0.32
	GF PA 12-FR PA	0.11	GF PA 12-FR PA 11	0.1	GF PA 12-FR PA 11	0.13	GF PA 12-FR PA 11	0.16
	I-E	0.04					I-E	0.05

Table 31: Hole accuracy mean differences

Hole Accuracy														
Wall Thickness (mm)														
	1.0		2.5		4.0		5.5		7.0		8.5		10.0	
2.6mm Hole	PA 12-GF PA 12	0.26	PA 12-GF PA 12	0.32	PA 12-GF PA 12	0.29	PA 12-GF PA 12	0.31	PA 12-GF PA 12	0.26	PA 12-FR PA 11	0.32	PA 12-FR PA 11	0.29
	PA 12-FR PA 11	0.2	PA 12-FR PA 11	0.32	PA 12-FR PA 11	0.31	PA 12-FR PA 11	0.28	PA 12-FR PA 11	0.29	XY-YZ	0.37	XY-YZ	0.27
	XY-YZ	0.26	XY-YZ	0.35	XY-YZ	0.37	XY-YZ	0.35	XY-YZ	0.31	XZ-YZ	0.26	XZ-YZ	0.27
	XZ-YZ	0.25	XZ-YZ	0.32	XZ-YZ	0.34	XZ-YZ	0.3	XZ-YZ	0.27				
2.4mm Hole	PA 12-GF PA 12	0.24	PA 12-GF PA 12	0.22	PA 12-GF PA 12	0.2	PA 12-GF PA 12	0.28	PA 12-GF PA 12	0.22	PA 12-FR PA 11	0.32	PA 12-FR PA 11	0.2
	PA 12-FR PA 11	0.19	PA 12-FR PA 11	0.22	PA 12-FR PA 11	0.21	PA 12-FR PA 11	0.26	XY-YZ	0.33	XY-YZ	0.38	PA 12-FR PA 11	0.3
	XY-YZ	0.29	XY-YZ	0.36	XY-YZ	0.31	XY-YZ	0.3	XZ-YZ	0.31			XY-YZ	0.31
	XZ-YZ	0.28	XZ-YZ	0.32	XZ-YZ	0.32	XZ-YZ	0.33					XZ-YZ	0.35
				I-E	0.13									

Table 32: Thin wall accuracy mean differences

		Thin Wall Accuracy Wall Thickness (mm)														
		0.2		0.3		0.4		0.5		0.6		0.7		0.8		
Thin Wall - Outer	PA 12-GF PA 12	-0.11	PA 12-GF PA 12	-0.15	PA 12-GF PA 12	-0.18	PA 12-FR PA 11	-0.19	PA 12-GF PA 12	-0.09	PA 12-GF PA 12	-0.07	PA 12-GF PA 12	-0.07	PA 12-GF PA 12	-0.07
	PA 12-FR PA 11	-0.26	PA 12-FR PA 11	-0.23	PA 12-FR PA 11	-0.24	GF PA 12-FR PA 11	-0.17	PA 12-FR PA 11	-0.2	PA 12-FR PA 11	-0.21	PA 12-FR PA 11	-0.21	PA 12-FR PA 11	-0.22
	GF PA 12-FR PA	-0.15	XY-XZ	-0.12	XY-XZ	-0.09	XY-XZ	-0.07	GF PA 12-FR PA 11	-0.11	GF PA 12-FR PA 11	-0.14	GF PA 12-FR PA 11	-0.14	GF PA 12-FR PA 11	-0.15
	XY-YZ	-0.14	XY-YZ	-0.15	XY-YZ	-0.14	XY-YZ	-0.11	XY-XZ	-0.07	XY-YZ	-0.13	XY-YZ	-0.13	XY-YZ	-0.11
			IE	-0.07			IE	-0.04	XY-YZ	-0.17	XZ-YZ	-0.1	XZ-YZ	-0.09		
Thin Wall - Middle	PA 12-GF PA 12	-0.09	PA 12-GF PA 12	-0.13	PA 12-GF PA 12	-0.15	PA 12-FR PA 11	-0.18	PA 12-GF PA 12	-0.08	PA 12-GF PA 12	-0.06	PA 12-GF PA 12	-0.06	PA 12-GF PA 12	-0.06
	PA 12-FR PA 11	-0.22	PA 12-FR PA 11	-0.2	PA 12-FR PA 11	-0.23	GF PA 12-FR PA 11	-0.17	PA 12-FR PA 11	-0.2	PA 12-FR PA 11	-0.21	PA 12-FR PA 11	-0.21	PA 12-FR PA 11	-0.22
	GF PA 12-FR PA	-0.13	GF PA 12-FR PA	-0.07	XY-XZ	-0.1	XY-XZ	-0.1	GF PA 12-FR PA 11	-0.11	GF PA 12-FR PA 11	-0.15	GF PA 12-FR PA 11	-0.15	GF PA 12-FR PA 11	-0.16
	XY-XZ	-0.12	XY-XZ	-0.16	XY-YZ	-0.12	XY-YZ	-0.09	XY-XZ	-0.09	XY-YZ	-0.1	XY-YZ	-0.1	XY-YZ	-0.09
			XY-YZ	-0.11	XY-YZ	-0.12			XY-YZ	-0.13	XZ-YZ	-0.06				

References

- [1] Gideon N. Levy, Ralf Schindel, J.P. Kruth, "Rapid manufacturing and rapid tooling with layer manufacturing (LM) technologies, state of the art and future perspectives," *CIRP Annals - Manufacturing Technology*, vol. 52, no. 2, pp. 589-609, 2003.
- [2] "ALM materials, processes, and economics," Asociatia Techsoup Romania, Bucharest, 2012.
- [3] Terry Wohlers, Tim Caffrey, Wohlers Report 2015, Fort Collins, CO: Wohlers Associates, Inc, 2015.
- [4] Ian Gibson, Shi Dongping, "Material properties and fabrication parameters in selective laser sintering process," *Rapid Prototyping Journal*, vol. 3, no. 4, pp. 129-135, 1997.
- [5] "Laser Sintering," Design, Research, and Education for Additive Manufacturing Systems, [Online]. Available: <http://seb199.me.vt.edu/dreams/laser-sintering/>. [Accessed 16 April 2017].
- [6] M. Mahesh, Y.S. Wong, J.Y.T. Fug, H.T. Loh, "Benchmarking for comparative evaluation of RP systems and processes," *Rapid Prototyping Journal*, vol. 10, no. 2, pp. 123-135, 2004.
- [7] L. Castillo, "Study about the rapid manufacturing of complex parts of stainless steel and titanium," TNO Industrial Technology, 2005.

- [8] Tyler Govett, Kevin Kim, Michael Lundin, Daniel Pinero, "Design Rules for Selective Laser Sintering," in *SFF Symposium*, Austin, TX, 2012.
- [9] Shawn Moylan, John Slotwinski, April Cooke, Kevin Jurrens, M. Alkan Donmez, "An Additive Manufacturing Test Artifact," *Journal of Research of the National Institute of Standards and Technology*, vol. 119, pp. 429-459, 2014.
- [10] J. Allison, C. Sharpe, C. Seepersad, "A Test Part for Evaluating the Accuracy and Resolution of a Polymer Powder Bed," *Journal of Mechanical Design*, 2017. In Press.
- [11] "3D Systems Offers Manufacturing-Capable Upgrade Package to Legacy SLS Systems," *Business Wire*, 10 September 2004. [Online]. Available: <http://www.businesswire.com/news/home/20040910005184/en/3D-Systems-Offers-Manufacturing-Capable-Upgrade-Package-Legacy>. [Accessed 16 April 2017].
- [12] David L Bourell, Ming C. Leu, David W. Rosen, "Roadmap for Additive Manufacturing," Washington D.C., 2009.
- [13] J.P. Kruth, X. Wang, T. Laoui, L. Froyen, "Lasers and materials in selective laser sintering," *Assembly Automation*, vol. 23, no. 4, pp. 357-371, 2003.
- [14] AZO Materials, "Polyamide 11-Nylon 11-PA 11 Fire Retardant," AZO Materials, 12 May 2001. [Online]. Available: <http://www.azom.com/article.aspx?ArticleID=438>. [Accessed 16 April 2017].

- [15] R.D. Goodridge, C.J. Tuck, R.J.M. Hague, "Laser sintering of polyamides and other polymers," *Progress in Materials Science*, vol. 57, pp. 229-267, 2012.
- [16] U. Ajoku, N. Saleh, N. Hopkinson, R. Hague, P. Erasenthiran, "Investigating mechanical anisotropy and end-of-vector effect in laser-sintered nylon parts," *Proceedings of the Institution of Mechanical Engineers*, vol. 220, no. 7, pp. 1077-1086, 2006.
- [17] Cooke, W., Tomlinson, R.A., Burguete, R., Johns, D., Vanard, G., "Anisotropy, homogeneity and ageing in an SLS polymer," *Rapid Prototyping Journal*, vol. 17, no. 4, pp. 269-279, 2011.
- [18] B. Caulfield, P.E. McHugh, S. Lohfeld, "Dependence of mechanical properties of polyamide components on build parameters in the SLS process," *Journal of Materials Processing Technology*, vol. 182, pp. 477-488, 2007.
- [19] David L. Bourell, Trevor J. Watt, David K. Leigh, Ben Fulcher, "Performance limitations in polymer laser sintering," *Physics Procedia*, vol. 56, pp. 147-156, 2014.
- [20] Woodall, W.H., Borrer, C.M., "Some Relationships Between Gage R&R Criteria," *Quality and Reliability Engineering International*, vol. 24, pp. 99-106, 2008.
- [21] Geoffrey Boothroyd, Peter Dewhurst, Winstin A. Knight, *Product Design for Manufacturing and Assembly*, Third Edition, Boca Raton: CRC Press, 2011.
- [22] D. Sippel, "Investigation of detail resolution on basic shapes and development of design rules," EOS e-Manufacturing Solutions, 2008.

- [23] J. Cheng, S. Lao, W. Ho, A. Cummings, and J. Koo, "SLS Processing of Nylon 11 Nanocomposites," in *SFF Symposium*, Austin, TX, 2005.